strain HIV-1 but did not inhibit the X4 strain HIV-1 (Table I). These results suggest that YM-370749 inhibited HIV-1 replication by inducing CCR5 internalization and/or inhibiting HIV binding. Although the extent of CCR5 internalization caused by YM-370749 in B300-19/CCR5 cells was modest (Fig. 4*B*), YM-370749 may induce CCR5 internalization more efficiently in PBM or NP-2 cells. Internalization of CCR5 has been reported to be affected by the expression levels of the cellular β-arrestins and G protein receptor kinase (26). Alternatively, the anti-HIV-1 activity might be attributable to the modest effect on CCR5 internalization. This is because the reduced expression level of CCR5 in *CCR5Δ32* heterozygotes is known to be responsible for the slower progression of HIV-1 infection (44). Alternatively, Reeves et al. (45) reported that cell susceptibility to R5 virus infection in other in vitro systems is unaffected by changes in CCR5 density >10-fold. Further study will be required to clarify whether the antiviral activity of YM-370749 is dependent on CCR5 internalization. The IC_{50} value (0.2 μM) obtained for the antiviral assay using PHAM-PBMC was lower than the IC_{50} values (0.5–1.5 μM) obtained for the antiviral assay using NP-2/CD4/CCR5-LTR-βGal cells and the EC_{50} values obtained for the functional assays using B300-19/CCR5 cells (2.1 and 1.4 μM for the $[Ca^{2+}]_i$ and GTPγS assays, respectively). Lengthy incubation periods with YM-370749 and/or a lower CCR5 density on the PBM cell surface compared with that on NP-2/CD4/CCR5-LTR-βGal cells and B300-19/CCR5 cells might cause a more effective down-modulation and/or occupation of CCR5 by YM-370749. However, cytotoxic (concentrations of 2.2 μM for PHAM-PBMC and 16 μM for NP-2/CD4/CCR5; see Table I), cytostatic, or other effects caused by YM-370749 might affect the antiviral activity. Further study will be required to clarify that the antiviral activity of YM-370749 is directly mediated through CCR5.

Structural analysis is useful for understanding the activation mechanism of CCR5 and for designing the novel anti-HIV-1 agent. The binding and $[Ca^{2+}]_i$ study using the I198M mutant clearly showed that Ile^{198} was involved in the interaction with YM-370749 (Table II and Fig. 6). Billick et al. (46) reported that I198M mutation abrogated HIV-1 entry inhibition by SCH-351125 and suggested that the region of CCR5 near Ile^{198} has an important influence on the conformational state of this receptor. It is tempting to speculate that interaction of YM-370749 with Ile^{198} induces a conformational change of CCR5 that leads to the activation.

Docking studies using YM-370749 and a three-dimensional model of CCR5 showed that the binding site of YM-370749 is located in a pocket surrounded by a transmembrane domain (Fig. 7, *A* and *B*). Considering that CCL5 interacts with the N-terminal extracellular domain and the second extracellular loop of CCR5 (47), our results suggest that the binding site of YM-370749 is quite different from that of CCL5, and it would explain the functional difference between YM-370749 and CCL5. The docking studies also pointed out that the binding of YM-370749 is mediated by an electrostatic interaction with Glu^{283} in TM-VII and by hydrophobic interactions with the Tyr^{108} and Phe^{109} in TM-III, Ile^{198} in TM-V, and Tyr^{251} in TM-VI on CCR5. Among the five amino acid residues at which we showed the interaction with YM-370749 in the docking studies, the Phe^{109} is not conserved in other chemokine receptor subtypes (Tyr in CCR1, His in CCR2 and CCR3, and Leu in CCR4). The Phe^{109} might therefore contribute to the chemokine receptor selectivity of YM-370749.

The Glu^{283} is well conserved among chemokine receptors and is involved in CCR5 antagonist binding (48, 49). Analogous glutamate residues within CCR1, CCR2, and CXCR4 have been shown to be important for small molecule antagonist binding (50–52). Our results suggest that YM-370749 also uses common electrostatic interactions between the antagonist and a common acidic amino acid in TM-VII of the receptors. The crystal structure of the transcription regulator BmrR complex with tetraphenylphosphonium, the structure of which is similar to that of YM-370749 (53), will explain that the positive charge on the phenyl ring in YM-370749 is due to the phosphorus atom and makes an electrostatic interaction with Glu^{283}.

Govaerts et al. (54, 55) has reported that mutations of Tyr^{108} and other aromatic residues located in CCR5 TM-II and TM-III differentially affected the functional response to various natural ligands without significantly altering their binding affinity and suggested that the amino acid residues were involved in the activation of the receptor. YM-370749 may exert its agonistic activity through the interaction with Tyr^{108}. Further studies will be needed to understand more precisely the molecular details of CCR5 active states induced by YM-370749.

In summary, YM-370749 is a small molecule, functionally selective agonist for the human CCR5 that can inhibit the replication of HIV-1. Insights into the molecular basis for the interaction of CCR5 with YM-370749 will provide structural basis for understanding the CCR5 activation mechanism and for designing ideal anti-HIV-1 agents that promote internalization of CCR5 without proinflammatory activity.

Acknowledgments

We thank Dr. Shigekazu Nagata (Osaka University, Osaka, Japan) for providing pEF-BOS and Dr. H. Hoshino (Gunma University, Maebashi, Japan) for providing the NP-2 cells derived from human glioma.

Disclosures

The authors have no financial conflict of interest.

References

1. Carpenter, C. C., M. A. Fischl, S. M. Hammer, M. S. Hirsch, D. M. Jacobsen, D. A. Katzenstein, J. S. Montaner, D. D. Richman, M. S. Saag, R. T. Schooley, et al. 1998. Antiretroviral therapy for HIV infection in 1998: updated recommendations of the International AIDS Society-USA panel. *J. Am. Med. Assoc.* 280: 78–86.
2. Montessori, V., N. Press, M. Harris, L. Akagi, and J. S. Montaner. 2004. Adverse effects of antiretroviral therapy for HIV infection. *Can. Med. Assoc. J.* 170: 229–238.
3. Siliciano, J. D., J. Kajdas, D. Finzi, T. C. Quinn, K. Chadwick, J. B. Margolick, C. Kovacs, S. J. Gange, and R. F. Siliciano. 2003. Long-term follow-up studies confirm the stability of the latent reservoir for HIV-1 in resting $CD4^+$ T cells. *Nat. Med.* 9: 727–728.
4. Strader, C. D., T. M. Fong, M. R. Tota, D. Underwood, and R. A. Dixon. 1994. Structure and function of G protein-coupled receptors. *Annu. Rev. Biochem.* 63: 101–132.
5. Alkhatib, G., C. Combadiere, C. C. Broder, Y. Feng, P. E. Kennedy, P. M. Murphy, and E. A. Berger. 1996. CC CKR5: a RANTES, MIP-1α, MIP-1β receptor as a fusion cofactor for macrophage-tropic HIV-1. *Science* 272: 1955–1958.
6. Deng, H., R. Liu, W. Ellmeier, S. Choe, D. Unutmaz, M. Burkhart, P. Di Marzio, S. Marmon, R. E. Sutton, C. M. Hill, et al. 1996. Identification of a major co-receptor for primary isolates of HIV-1. *Nature* 381: 661–666.
7. Choe, H., M. Farzan, Y. Sun, N. Sullivan, B. Rollins, P. D. Ponath, L. Wu, C. R. Mackay, G. LaRosa, W. Newman, et al. 1996. The β-chemokine receptors CCR3 and CCR5 facilitate infection by primary HIV-1 isolates. *Cell* 85: 1135–1148.
8. Feng, Y., C. C. Broder, P. E. Kennedy, and E. A. Berger. 1996. HIV-1 entry cofactor: functional cDNA cloning of a seven-transmembrane, G protein-coupled receptor. *Science* 272: 872–877.
9. Doranz, B. J., J. Rucker, Y. Yi, R. J. Smyth, M. Samson, S. C. Peiper, M. Parmentier, R. G. Collman, and R. W. Doms. 1996. A dual-tropic primary HIV-1 isolate that uses fusin and the β-chemokine receptors CKR-5, CKR-3, and CKR-2b as fusion cofactors. *Cell* 85: 1149–1158.
10. Dragic, T., V. Litwin, G. P. Allaway, S. R. Martin, Y. Huang, K. A. Nagashima, C. Cayanan, P. J. Maddon, R. A. Koup, J. P. Moore, and W. A. Paxton. 1996. HIV-1 entry into $CD4^+$ cells is mediated by the chemokine receptor CC-CKR-5. *Nature* 381: 667–673.
11. Liu, R., W. A. Paxton, S. Choe, D. Ceradini, S. R. Martin, R. Horuk, M. E. MacDonald, H. Stuhlmann, R. A. Koup, and N. R. Landau. 1996. Homozygous defect in HIV-1 coreceptor accounts for resistance of some multiply-exposed individuals to HIV-1 infection. *Cell* 86: 367–377.
12. Samson, M., F. Libert, B. J. Doranz, J. Rucker, C. Liesnard, C. M. Farber, S. Saragosti, C. Lapoumeroulie, J. Cognaux, C. Forceille, et al. 1996. Resistance

Novel HIV-1 Integrase Inhibitors Derived from Quinolone Antibiotics

Motohide Sato,† Takahisa Motomura,† Hisateru Aramaki,† Takashi Matsuda,† Masaki Yamashita,† Yoshiharu Ito,† Hiroshi Kawakami,† Yuji Matsuzaki,† Wataru Watanabe,† Kazunobu Yamataka,† Satoru Ikeda,† Eiichi Kodama,‡ Masao Matsuoka,‡ and Hisashi Shinkai*,†

Central Pharmaceutical Research Institute, JT Inc., 1-1 Murasaki-cho, Takatsuki, Osaka, 569-1125, Japan, and Institute for Virus Research, Kyoto University, 53 Shogoin Kawaramachi, Sakyo-ku, Kyoto, 606-8507, Japan

Received January 6, 2006

Abstract: The viral enzyme integrase is essential for the replication of human immunodeficiency virus type 1 (HIV-1) and represents a remaining target for antiretroviral drugs. Here, we describe the modification of a quinolone antibiotic to produce the novel integrase inhibitor JTK-303 (GS 9137) that blocks strand transfer by the viral enzyme. It shares the core structure of quinolone antibiotics, exhibits an IC_{50} of 7.2 nM in the strand transfer assay, and shows an EC_{50} of 0.9 nM in an acute HIV-1 infection assay.

Human immunodeficiency virus type 1 (HIV-1) integrase, along with HIV-1 reverse transcriptase and HIV-1 protease, is an essential enzyme for retroviral replication and represents an important target for interrupting the viral replication cycle.[1] HIV-1 integrase first catalyzes removal of the terminal dinucleotide from each 3′-end of viral DNA (3′-processing) and subsequently mediates joining of the 3′-end of the viral DNA to host DNA (strand transfer).[2] Reverse transcriptase inhibitors and protease inhibitors have already made significant advances in antiretroviral therapy but cannot achieve complete suppression and risk producing resistant HIV-1.[3,4] On the other hand, despite numerous attempts to develop integrase inhibitors, only the diketo acid class of compounds is at an advanced stage of development and no integrase inhibitors have yet been approved for therapeutic use.[1,5−7] Here, we report that the core structure of quinolone antibiotics can be used as an alternative to the diketo acid class of HIV-1 integrase inhibitors and how this finding led to a novel quinolone integrase inhibitor, JTK-303 (GS 9137).

The diketo acid moiety (γ-ketone, enolizable α-ketone, and carboxylic acid) was believed to be essential for the inhibitory activity of this series of integrase inhibitors,[8] and the structures of diketotriazole **2**,[6] diketotetrazole **3**,[9] diketopyridine **4**,[10] and 7-carbonyl-8-hydroxy-(1,6)-naphthyridine **5** [7,11] were reported to be bioisosters of the diketo acid pharmacophore (Figure 1). The carboxylic acid could be replaced with not only acidic bioisosters, such as tetrazole and triazole, but also by a basic heterocycle bearing a lone pair donor atom, such as a pyridine ring. It has been reported that the heteroaromatic nitrogen in the pyridine ring mimics the corresponding carboxyl oxygen in the diketo acid as a Lewis base equivalent.[11] The enolizable ketone at the α-position of diketo acids can be replaced with a phenolic hydroxyl group, indicating that the α-enol form of each diketo acid is its biologically active coplanar conformation.[11]

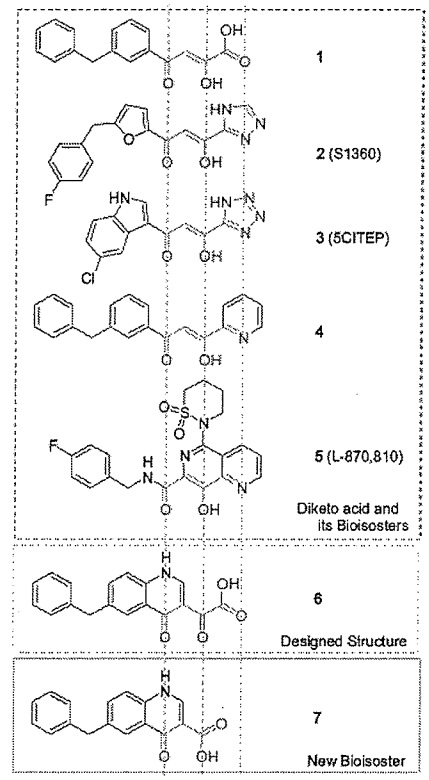

Figure 1. Structures of the diketo acid family and its new bioisoster.

All bioisosters of the diketo acid motif have the three functional groups that mimic a ketone, enolizable ketone, and carboxyl oxygen and can have a coplanar conformation (Figure 1). Therefore, we designed the structure of 4-quinolone-3-glyoxylic acid **6** as a new scaffold that maintained the coplanarity of diketo acid functional groups (Figure 1). Interestingly, not the 4-quinolone-3-glyoxlic acid **6** but its precursor 4-quinolone-3-carboxylic acid **7** showed integrase inhibitory activity. The 4-quinolone-3-carboxylic acid **7** only had two functional groups, a β-ketone and a carboxylic acid, which were coplanar. This result showed that the coplanar monoketo acid motif in 4-quinolone-3-carboxylic acid **7** could be an alternative to the diketo acid motif and provided novel insight into the structural requirements and the binding mode of this type of inhibitor. Quinolone **7** had an IC_{50} of 1.6 μM in the strand transfer assay, and structural modification of **7** led to a far more potent integrase inhibitor **12** with stronger antiviral activity (Table 1). Introduction of 2-fluoro and 3-chloro substituents into the distal benzene ring of **7** (**8**) led to a significant improvement of its inhibition of strand transfer (IC_{50} = 44 nM) and to the appearance of antiviral activity (EC_{50} = 0.81 μM). Compound **9**, bearing a hydroxyethyl group at the 1-position of the quinolone ring, was 1.8-fold more potent at inhibiting strand transfer (IC_{50} = 24 nM) and displayed about 11-fold stronger antiviral activity (EC_{50} = 76 nM) than **8**. Introduction of a methoxy group at the 7-position of the quinolone ring of **9** (**10**) led to a significant improvement of its inhibition of strand transfer (IC_{50} = 9.1 nM) and of antiviral activity (EC_{50} = 17.1 nM). Compound **11**, bearing an isopropyl group at the 1*S*-position of the hydroxyethyl moiety, was about 3-fold more potent at inhibiting strand transfer (IC_{50} = 8.2 nM) and about 10-fold stronger at inhibiting HIV

* To whom correspondence should be addressed. Phone: +81 72 681 9700. Fax: +81 72 681 9725. E-mail: hisashi.shinkai@ims.jti.co.jp.
† JT Inc.
‡ Kyoto University.

10.1021/jm0600139 CCC: $33.50
Published on Web 02/15/2006

Table 1. Summary of the Structural Optimization Process for Quinolone Integrase Inhibitors[e]

	compd	Inhibition of Strand Transfer[a] IC_{50} (nM)	Antiviral Activity[b] EC_{50} (nM)	Cytotoxicity (μM)
7	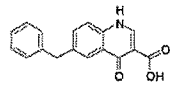	1600 ± 300	> 30000	> 30
8	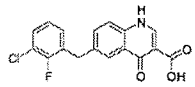	43.5 ± 8.8	805.2 ± 225.0	> 12
9	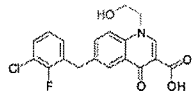	24.2 ± 11.6	76.3 ± 3.7	> 15
10	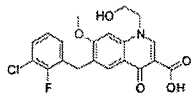	9.1 ± 2.1	17.1 ± 2.9	5.3 ± 1.1
11	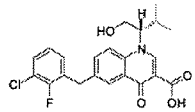	8.2 ± 1.7	7.5 ± 0.8	14.0 ± 2.0
12	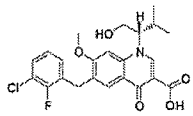	7.2 ± 2.2	0.9 ± 0.4	4.0 ± 0.8
5 (L-870,810)[c]		22.8 ± 4.3	3.6 ± 0.4	0.7 ± 0.06
Ciprofloxacin[d]		> 100000	–	–

[a] The strand transfer assay was performed according to the method of Hazuda[14] with some modifications.[15] [b] Antiviral activity was measured by the acute HIV-1 infection assay[16] with some modifications.[17] [c] Prepared according to the reported method.[18] [d] Available from Wako Pure Chemical [e] Data are given as the mean ± SD (n = 3).

replication (EC_{50} = 7.5 nM) than **9**, although introduction of an isopropyl group at the 1*R*-position of the hydroxyethyl moiety could not enhance inhibitory acitivity. Introduction of both a methoxy group at the 7-position of the quinolone ring and an isopropyl group at the 1*S*-position of the hydroxyethyl moiety of **9** (**12**) led to a synergistic improvement of antiviral acitivity (EC_{50} = 0.9 nM), but there was no additive or synergistic improvement in the inhibition of HIV-1 integrase (IC_{50} = 7.2 nM). This may be due to the condition of the strand transfer assay using 5 nM of target DNA that influences potencies of inhibitors.

Preparation of the quinolone analogues (**7**−**12**) is shown in Scheme 1. Palladium-catalyzed coupling of 3-chloro-2-fluorobenzylzinc bromide **13**, which was derived from the corresponding benzylbromide, with 1-iodo-4-nitrobenzene or 1-iodo-2-methoxy-4-nitrobenzene (Negishi coupling) and subsequent reduction of the nitro group gave the aniline **15** or **16**. Condensation of **15**, **16**, or commercially available **14** with diethyl ethoxymethylenemalonate and subsequent thermal cyclization of the aminoacrylate products in diphenyl ether led to the quinolone esters **17**, **18** and **19**.[19] Hydrolysis of **17** and **18** gave **7** and **8**, respectively. N-Alkylation of **18** or **19** with the *tert*-butyldimethylsilyl (TBS) ether of 2-hydroxyethylbromide and subsequent hydrolysis of the ethyl ester and TBS ether resulted in **9** or **10**. After 5-iodonation of 2-fluorobenzoic acids **20** and **21**, the acid chlorides of **20** and **21** were coupled with ethyl 3-(dimethylamino)acrylate to produce the acrylates **22** and

Scheme 1[a]

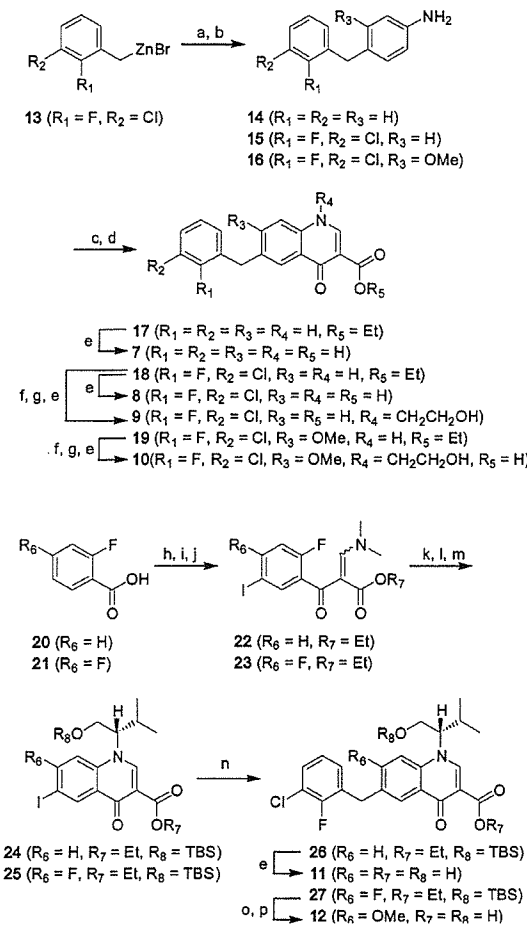

[a] Reagents and conditions: (a) 1-iodo-4-nitrobenzene, $PdCl_2(Ph_3P)_2$, THF, reflux; (b) Zn, AcOH; (c) diethyl ethoxymethylenemalonate, toluene, reflux; (d) Ph_2O, 250 °C; (e) NaOH, EtOH/H_2O, reflux; (f) $TBSOCH_2CH_2Br$, K_2CO_3, DMF, 80 °C; (g) TBAF, THF; (h) NIS, H_2SO_4; (i) $SOCl_2$, DMF, toluene, reflux; (j) ethyl 3-(dimethylamino)acrylate, THF, 50 °C; (k) (*S*)-valinol, THF; (l) K_2CO_3, DMF, 70 °C; (m) TBSCl, imidazole, DMF; (n) **13**, $Pd(dba)_2$, trifurylphosphine, THF, reflux; (o) NaOH, *i*-PrOH/H_2O, reflux; (p) NaOMe, MeOH, reflux.

23, respectively. Substitution with (*S*)-valinol and subsequent cyclization with potassium carbonate and protection of the alcohol with TBS ether gave the quinolones **24** and **25**, respectively.[20] Negishi coupling of **24** and **25** with **13** led to the quinolone esters **26** and **27**, respectively. Hydrolysis of **26** gave **11**. Hydrolysis of **27** and subsequent methoxylation with sodium methoxide produced **12**.

In summary, modification of quinolone antibiotics, which did not show HIV-1 integrase inhibitory activity (Table 1), led to discovery of the coplanar monoketo acid motif in their scaffold, 4-quinolone-3-carboxylic acid, as an alternative to the diketo acid motif. These novel quinolone integrase inhibitors were structurally optimized in the highly potent **12**, which had little antibacterial activity although it still retained the core structure of quinolone antibiotics. Compound **12** was much more potent at inhibiting integrase-catalyzed strand transfer processes than 3′-processing reactions, as previously reported for compounds of the diketo acid class.[12,13] This indicates that it probably inhibits HIV-1 integrase via a mechanism similar to that of diketo acids, although there is no direct evidence (such as cocrystal data) that the coplanar monoketo acid motif shows the same mode of binding to the enzyme as the diketo acid

motif. Clinical studies of the novel quinolone integrase inhibitor **12** (GS 9137) are currently being conducted by Gilead Sciences.

Acknowledgment. We thank H. Isoshima and K. Kondo for sample preparation; S. Kato for comments on the manuscript; and S. Ishiguro, J. Haruta, and M. Kano for support.

Supporting Information Available: Analytical data for **5** and **7**−**12**. This material is available free of charge via the Internet at http://pubs.acs.org.

References

(1) Pommier, Y.; Johnson, A. A.; Marchand, C. Integrase inhibitors to treat HIV/AIDS. *Nat. Rev. Drug Discovery* **2005**, *4*, 236−248.
(2) Craigie, R. HIV integrase, a brief overview from chemistry to therapeutics. *J. Biol. Chem.* **2001**, *276*, 23213−23215.
(3) Richman, D. D. HIV chemotherapy. *Nature* **2001**, *410*, 995−1001.
(4) Weiss, R. A. HIV and AIDS: looking ahead. *Nat. Med.* **2003**, *9*, 887−891.
(5) Johnson, A. A.; Marchand, C.; Pommier, Y. HIV-1 integrase inhibitors: a decade of research and two drugs in clinical trial. *Curr. Top. Med. Chem.* **2004**, *4*, 1059−1077.
(6) Barreca, M. L.; Ferro, S.; Rao, A.; Luca, L. D.; Zappala, M.; Monforte, A. M.; Debyser, Z.; Witvrouw, M.; Chimirri, A. Pharmacophore-based design of HIV-1 integrase strand-transfer inhibitors. *J. Med. Chem.* **2005**, *48*, 7084−7088.
(7) Hazuda, D. J.; Young, S. D.; Guare, J. P.; Anthony, N. J.; Gomez, R. P.; Wai, J. S.; Vacca, J. P.; Handt, L.; Motzel, S. L.; Klein, H. J.; Dornadula, G.; Danovich, R. M.; Witmer, M. V.; Wilson, K. A. A.; Tussey, L.; Schleif, W. A.; Gabryelski, L. S.; Jin, L.; Miller, M. D.; Casimiro, D. R.; Emini, E. A.; Shiver, J. W. Integrase inhibitors and cellular immunity suppress retroviral replication in rhesus macaques. *Science* **2004**, *305*, 528−532.
(8) Grobler, J. A.; Stillmock, K.; Binghua, H.; Witmer, M.; Felock, P.; Espeseth, A. S.; Wolfe, A.; Egbertson, M.; Bourgeois, M,; Melamed, J.; Wai, J. S.; Young, S.; Vacca, J.; Hazuda, D. J. Diketo acid inhibitor mechanism and HIV-1 integrase: implications for metal binding in the active site of phosphotransferase enzymes. *Proc. Natl. Acad. Sci. U.S.A.* **2002**, *99*, 6661−6666.
(9) Goldgur, Y.; Craigie, R.; Cohen, G. H.; Fujiwara, T.; Yoshinage, T.; Fujishita, T.; Sugimoto, H.; Endo, T.; Murai, H.; Davies, D. R. Structure of the HIV-1 integrase catalytic domain complexed with an inhibitor: a platform for antiviral drug design. *Proc. Natl. Acad. Sci. U.S.A.* **1999**, *96*, 13040−13043.
(10) Hazuda, D. J.; Anthony, N. J.; Gomez, R. P.; Jolly, S. M.; Wai, J. S.; Zhuang, L.; Fisher, T. E.; Embrey, M.; Guare, J. P., Jr.; Egbertson, M. S.; Vacca, J. P.; Huff, J. R.; Felock, P. J.; Witmer, M. V.; Stillmock, K. A.; Danovich, R.; Grobler, J.; Miller, M. D.; Espeseth, A. S.; Jin, L.; Chen, I. W.; Lin, J. H.; Kassahun, K.; Ellis, J. D.; Wong, B. K.; Xu, W.; Pearson, P. G.; Schleif, W. A.; Cortese, R.; Emini, E.; Summa, V.; Holloway, M. K.; Young, S. D. A naphthyridine carboxamide provides evidence for discordant resistance between mechanistically identical inhibitors of HIV-1 integrase. *Proc. Natl. Acad. Sci. U.S.A.* **2004**, *101*, 11233−11238.
(11) Zhuang, L.; Wai, J. S.; Embrey, M. W.; Fisher, T. E.; Egbertson, M. S.; Payne, L. S.; Guare, J. P., Jr.; Vacca, J. P.; Hazuda, D. J.; Felock, P. J.; Wolfe, A. L.; Stillmock, K. A.; Witmer, M. V.; Moyer, G.; Schleif, W. A.; Gabryelski, L. J.; Leonard, Y. M.; Lynch, J. J., Jr.; Michelson, S. R.; Young, S. D. Design and synthesis of 8-hydroxy-[1,6]naphthyridines as novel inhibitors of HIV-1 integrase in vitro and in infected cells. *J. Med. Chem.* **2003**, *46*, 453−456.
(12) Hazuda, D. J.; Felock, P.; Witmer, M.; Wolfe, A.; Stillmock, K.; Grobler, J. A.; Espeseth, A.; Gabryelski, L.; Schleif, W.; Blau, C.; Miller, M. D. Inhibitors of strand transfer that prevent integration and inhibit HIV-1 replication in cells. *Science* **2000**, *287*, 646−650.
(13) Sechi, M.; Derudas, M.; Dallocchio, R.; Dessi, A.; Bacchi, A.; Sannia, L.; Carta, F.; Palomba, M.; Ragab, O.; Chan, C.; Shoemaker, R.; Sei, S.; Dayam, R.; Neamati, N. Design and synthesis of novel indole β-diketo acid derivatives as HIV-integrase inhibitors, *J. Med. Chem.* **2004**, *47*, 5298−5310.
(14) Hazuda, D. J.; Hastings, J. C.; Wolfe, A. L.; Emini, E. A. A novel assay for the DNA strand-transfer reaction of HIV-1 integrase. *Nucleic Acids Res.* **1994**, *22*, 1121−1122.
(15) Donor DNA (which was processed at the 3′ end of the strand and biotinylated at the 5′ end) was immobilized on streptavidin-coated microtiter plates. Recombinant integrase (300 nM) was assembled on the immobilized donor DNA (0.5 pmol per well) in 100 μL of reaction buffer (30 mM 3-(*N*-morpholino)propanesulfonic acid (MOPS), 5 mM $MgCl_2$, 3 mM dithiothreitol (DTT), 0.1 mg/mL bovine serum albumin (BSA), 5% glycerol, 10% DMSO, 0.01% Tween-20) by incubation for 60 min at 37 °C. Then excess enzyme was removed and a test compound was added. The strand transfer reaction was initiated by addition of target DNA (5 nM), which was labeled at the 3′ end with digoxigenin. After incubation at 37 °C for 10 min, the plates were washed with phosphate-buffered saline (PBS) containing 0.1% Tween-20. The digoxigenin-labeled products were detected using anti-digoxigenin-peroxidase (POD) Fab fragments (Roche Diagnostics) and a POD substrate, tetramethylbenzidine (TMB). Then 100 μL of anti-digoxigenin-POD Fab fragment solution was added to each well, and the plates were incubated at 37 °C for 60 min. After the mixture was washed with PBS containing 0.1% Tween-20, 100 μL of the POD substrate (TMB) was added to each well, and the plates were incubated at room temperature. The colorimetric reaction was stopped by addition of 100 μL of 0.5 M H_2SO_4, and the absorbance was measured at 450 nm by a microplate reader (SPECTRA max 340, Molecular Devices).
(16) Pauwels, R.; Balzarini, J.; Baba, M.; Snoeck, R.; Schols, D.; Herdewijn, P.; Desmyter, J.; De Clercq, E. Rapid and automated tetrazolium-based colorimetric assay for the detection of anti-HIV compounds. *J. Virol. Methods* **1988**, *20*, 309−321.
(17) MT-4 human T lymphoid cells (1×10^5 cells/mL) in RPMI 1640 medium containing 10% fetal bovine serum, 100 U/mL penicillin, and 100 μg/mL streptomycin were infected with HIV-1 strain IIIb at a multiplicity of 0.01 and were distributed into 96-well microtiter plates. Test compounds were added to the wells, and cultures were incubated at 37 °C for 5 days. Cell viability was determined by the MTT assay, which measures living cells on the basis of mitochondrial dehydrogenase activity. The cells were incubated with 3-(4,5-dimethylthiazol-2-yl)-2,5-diphenyltetrazolium bromide (MTT) solution (7.5 mg/mL). The MTT formazan crystals were dissolved in acidic 2-propanol containing 4% Triton-X, and the absorbance was measured at 595 nm.
(18) Anthony, N. J.; Gomez, R. P.; Young, S. D.; Egbertson, M.; Wai, J. S.; Zhuang, L.; Embrey, M.; Tran, L.; Melamed, J. Y.; Langford, H. M.; Guare, J. P.; Fisher, T. E.; Jolly, S. M.; Kuo, M. S.; Perlow, D. S.; Bennett, J. J.; Funk, T. W. Aza- and polyaza-naphthalenyl carboxamides useful as HIV integrase inhibitors. PCT Int. Appl. WO02/30930 A2, 2002 (Merck & Co., Inc.).
(19) Gould, R. G., Jr.; Jacobs, W. A. The synthesis of certain substituted quinolines and 5,6-benzoquinolines. *J. Am. Chem. Soc.* **1939**, *61*, 2890−2895.
(20) Cecchetti, V.; Fravolini, A.; Lorenzini, M. C.; Tabarrini, O.; Terni, P.; Xin, T. Studies on 6-aminoquinolones: synthesis and antibacterial evaluation of 6-amino-8-methylquinolones. *J. Med. Chem.* **1996**, *39*, 436−445.

JM0600139

Nucleic Acids Symposium Series No. 50 1–2
doi:10.1093/nass/nrl001

2'-Deoxy-4'-*C*-ethynyl-2-fluoroadenosine: A nucleoside reverse transcriptase inhibitor with highly potent activity against all HIV-1 strains, favorable toxic profiles and stability in plasma

Hiroshi Ohrui[1], Satoru Kohgo[2], Hiroyuki Hayakawa[2], Eiichi Kodama[3], Masao Matsuoka[3], Tomohiro Nakata[4] and Hiroyuki Mitsuya[4,5]

[1]Yokohama College of Pharmacy, Yokohama, Japan, [2]Yamasa Corporation, Chiba, Japan, [3]Institute for Virus Research, Kyoto, Japan, [4]Kumamoto University, School of Medicine, Kumamoto, Japan and [5]National Cancer Institute/National Institute of Health, Bethesda, Maryland, USA

ABSTRACT

A working hypothesis to solve the critical problems of existing HAART was proposed. The study based on the hypothesis proved the validity of the hypothesis and resulted in the development of 2'-deoxy-4'-*C*-ethynyl-2-fluoro-adenosine (4'Ed2FA), a nucleoside reverse transcriptase inhibitor (NRTI) with highly potent activity against all HIV-1 strains, very favourable toxic profiles, and stability in plasma.

INTRODUCTION

HAART has dramatically improved the q. o. l. and prognosis of patients infected with HIV-1. However, the existing HAART has critical problems. They are
1) emergence of drug-resistant HIV variants,
2) requirement of frequent and large doses of drugs,
3) side effects of drugs.
A working hypothesis to solve the problems was proposed based on the fundamentals of both organic chemistry and biochemistry, and past findings of relationship between biological activity and structure of nucleoside derivatives. The hypothesis is comprised of the following three ways.

1) The way to prevent emergence of drug-resistant HIV
All clinical **NRTIs** belong to the family of 2',3'-dideoxy-nucleoside (**ddN**). The **ddN** structure has been assumed essential for nucleoside derivative to be anti-HIV active, i.e. to be the chain terminator of proviral DNA biosynthesis. However, HIV variants resistant to all these clinical **NRTIs** emerged. Resistance to these **ddNs** means that HIV can acquire the ability to discriminate between **ddN** and physiologic 2'-deoxynucleoside (**dN**) and does not accept **ddN** into the active center of its reverse transcriptase (**RT**) and /or selectively cut off the incorporated **ddN** from its proviral DNA terminus. Thus, resistance is the discrimination by HIV. Therefore, the nucleoside (**N**) that could prevent the emergence of drug-resistant HIV variants must satisfy the following conditions.

(1) To prevent discrimination by HIV, **N** must have the structure very much like **dN**. Therefore, **N** must have 3'-OH.
(2) In spite of having 3'-OH, **N** must be the chain terminator of proviral DNA biosynthesis.
2'-deoxy-4'-*C*-substitutednucleoside (**4'SdN**) was designed as the nucleoside that can satisfy these conditions on the basis of the following hypothesis.
(a) It will be difficult for HIV to discriminate between **4'SdN** and **dN** because **4'SdN** has all the functional groups of **dN**.
(b) The neopentyl-type secondary 3'-OH of **4'SdN** would be too unreactive to be used for elongation of proviral DNA biosynthesis. Thus, **4'SdN** could be the chain-terminator of proviral DNA biosynthesis.

2) The way to decrease the toxicity of nucleosides
In 1960s and 1970s, organic chemists synthesized nucleoside derivatives modified at two or more than two positions of physiologic nucleosides expecting to get nucleoside derivatives with excellent biological activity. However, none of them showed remarkable biological activity. These results suggested that the intracellular important enzymes do not recognize these modified nucleosides as their substrates. Therefore, the toxicity of **4'SdN** could be decreased by additional modification.

3) The way to provide nucleosides with stability to both enzymatic and acidic glycolysis
The lone pair of the ring oxygen plays an important role in both enzymatic and acidic glycolysis of nucleosides by participating to form an oxocarbonium ion. The steric hindrance between the 4'-substituent and 3'-OH of **4'SdN** changes the ring conformation into 3'-endo (N-type). It will be difficult for the lone pair of the ring oxygen of **4'SdN** with 3'-endo conformation to form oxocarbonium ion because the three bonds, C4-O-C1-C2, can not be co-planar easily. Thus, the introduction of a substituent at the 4'-position of nucleosides provide them with stability to both enzymatic and acidic glycolysis.

RESULTS AND DISCUSSION

Studies based on the hypothesis have proved the validity of the hypothesis. Optimization of the 4'-substituents, bases, and their combinations has resulted in the development of 2'-deoxy-4'-*C*-ethynyl-2-fluoroadenosine (**4'Ed2FA**, a nucleoside modified at two positions (4' and 2) of physiologic deoxyadenosine, which is highly active against all existing HIV strains has low toxicity, and is stable to both enzymatic and acidic glycolysis.

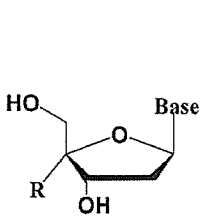

4'SdN

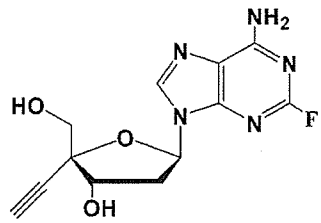

4'Ed2FA

The results of the biological evaluation of 4'Ed2FA

1) Anti-HIV activity:

EC_{50} (wild type)=0.2 nM; AZT=22 nM, (MDR)=0.14 nM; AZT=15,300 nM, (M184V)=3.1 nM; AZT=10 nM .

2) Toxicity:

DNA polymerase α: IC_{50}>200 μM,
DNA polymerase β: IC_{50}>200 μM,
Human mitochondrial DNA polymerase γ : IC_{50}=10 μM.
ddA: IC_{50}=0.2 μM
Mouse Toxicity: No acute toxicity up to 100 mg/kg by both oral and intravenous administration.

3) Stability to enzymatic and acidic glycolysis

Half life time of triphosphate of 4'Ed2FA: $T_{1/2}$: ~18hr,
triphosphate of AZT: $T_{1/2}$= 3hr

About 50% of the cells were protected against the infection of HIV-1 for 24 hr after removal of extracellular **4'Ed2FA** in both MT4 cells and MAGI cells cultured in the presence of 0.1 μM of **4'Ed2FA**.

Completely stable to adenosine deaminase under the conditions where **4'EdA** was completely deaminated within 60 min.

Only a small part (3 %) was hydrolyzed under the acidic Conditions of gastric juice (pH 1.06) at 24 °C, while **ddA** was completely decomposed in 5 min.

SUMMARY

A study on the synthesis and biological evaluation of **4'SdNs** was conducted according to a proposed hypothesis based on the fundamentals of both organic chemistry and biochemistry. Old findings proved the validity of the hypothesis and resulted in the development of **4'Ed2FA**, which is highly potent against all HIV-1s, is stable to intracellular catabolism and acidic degradation, has a very long intracellulat $T_{1/2}$, does not greatly inhibit DNA polymerase γ and does not have acute mouse toxicity. These results strongly suggest that **4'Ed2FA** deserves further study for the development of a highly potent therapeutic agent for HIV infection (**AIDS**), which may solve the problems of the existing HAART.

In addition, it should be noted that **4'Ed2FA** could be the ideal drug for both HIV and HBV infections. Hepatitis B virus (HBV) is a DNA virus, however, it also belongs to the family of retrovirus because it uses reverse transcriptase (**RT**) when it replicates. It was found that the **NRTIs** of HIV are also active against HBV, and **3TC** has been used for HBV infection.[9,10] However, HBV resistant to **3TC** has emerged. Since **4'Ed2FA** is highly active against 3TC-resistant HIV and will prevent the emergence of drug-resistant HIV, it is also expected to be active against drug-resistant HBV. Thus, **4'Ed2FA** could be the ideal drug for use against both HIV and HBV.

REFERENCES

1. Waga, T., Ohrui, H., Meguro, H. (1996) *Nucleosides Nucleotides,* **57,** 287.
2. Yamaguchi, T., Tomikawa, A., Hirai, T., Kawaguchi, T., Ohrui, H., Saneyoshi, M. (1997) *Nucleosides Nucleotides,* **16,** 1347.
3. Ohrui, H., Kohgo, S., Kitano, K., Sakata, S., Kodama, E., Yoshimura, K., Matsuoka, M., Shigeta, S., Mitsuya, H. (2001) *J. Med. Chem.*, **65,** 1879.
4. Kodama, E., Kohgo, S., Kitano, K., Machida, H., Gatanaga, H., Shigeta, S., Matsuoka, M., Ohrui, H., Mitsiya, H. (2001) *Antimicrobial Agents & Chemotherapy*, **45,** 1539.
5. Ohrui, H., Mitsuya, H. (2001) *Current Drug Targets-Infectious Disorder*, **1,** 1.
6. Kohgo, S., Yamada, K., Kitano, K., Iwai, Y., Sakata, N., Hayakawa, H., Nameki, D., Kodama, E., Matsuoka, M., Ohrui, H., Mitsuya, H. (2004) *Nucleosides Nucleotides*, **23,** 671.
7. Patent: International Publication Number, WO2005/090349, PCT/JP2005/005374
8. Nakata, H., Amano, M., Koh, Y., Kodama, E., Yang, G., Kohgo, S., Hayakawa, H., Ohrui, H., Matsuoka, M., Mitsuya, H. (2006) Abstract of 13th Conference on Retroviruses and Opportunistic Infections (CRO), F (antiviral therapy-preclinical), p219 (poster).
9. Lai, C. L., Dienstag, J., Schiff, E., Leung, N. W. Y., Akins, M., Hunt, C., Brown, N., Woessner, M., Boehme, R., Condreay, L. (2003) *Clin. Infect. Dis.*, **36,** 687.
10. Villeneuve, J. P., Durantel, D., Durantel, S., Westland, C., Xiong, S., Brosgart, C. L., Bibbs, C. S., Parvas, P., Nerle, B., Trepo, C., Zoulim, F. J. (2003) *Heptol.*, **39,** 1085.

JOURNAL OF VIROLOGY, Jan. 2005, p. 764–770 Vol. 79, No. 2
0022-538X/05/$08.00+0 doi:10.1128/JVI.79.2.764–770.2005

Mutations Conferring Resistance to Human Immunodeficiency Virus Type 1 Fusion Inhibitors Are Restricted by gp41 and Rev-Responsive Element Functions

Daisuke Nameki,[1] Eiichi Kodama,[1]* Mieko Ikeuchi,[1] Naoto Mabuchi,[2] Akira Otaka,[3] Hirokazu Tamamura,[3] Mutsuhito Ohno,[2] Nobutaka Fujii,[3] and Masao Matsuoka[1]

Laboratory of Virus Immunology[1] and Laboratory of Biochemistry,[2] Institute for Virus Research, Graduate School of Pharmaceutical Science,[3] Kyoto University, Kyoto, Japan

Received 24 May 2004/Accepted 27 August 2004

One of the human immunodeficiency virus (HIV) envelope proteins, gp41, plays a key role in HIV fusion. A gp41-derived peptide, T-20, efficiently inhibits HIV fusion and is currently approved for treatment of HIV-infected individuals. Although resistant variants have been reported, the mechanism of the resistance remains to be defined. To elucidate the mechanism in detail, we generated variants resistant to C34, a peptide derived from the gp41 carboxyl terminus heptad repeat (C-HR) in vitro. The resistant variants had a 5-amino-acid deletion in gp120 and a total of seven amino acid substitutions in gp41. Binding assays revealed that an I37K substitution in the N-terminal heptad repeat (N-HR) impaired the binding of C34, whereas an N126K substitution in the C-HR enhanced the binding to mutated N-HR, indicating that both mutations were directly involved in resistance. On the other hand, substitutions for A30 and D36 seemed to be secondary mutations, located complementary to each other in the Rev-responsive element (RRE), and were mutated simultaneously to maintain the secondary structure of the RRE that was impaired by the mutations at I37. Thus, HIV acquired resistance to C34 by mutations in N-HR, which directly interacted with C34. However, since this region also encoded the RRE, additional mutations were required to maintain viral replication. These results suggest that HIV fusion is one of the attractive targets for HIV chemotherapy.

Peptide inhibitors that block human immunodeficiency virus type 1 (HIV-1) fusion were first reported by Wild et al. (30). Recently, a peptide fusion inhibitor (T-20 or enfuvirtide) has been approved in the United States and Europe for treatment of HIV-infected individuals. The peptide sequence of T-20 is derived from the gp41 C terminus heptad repeat (C-HR) sequence, which corresponds to a linear region of 36 amino acids, and T-20 inhibits fusion by binding to the N-terminal heptad repeat (N-HR) of gp41 and preventing 6-helix bundle formation (4, 30). In HIV-infected patients, the effect of T-20 in combination with an antiretroviral regimen that was optimized with the aid of phenotypic and genotypic resistance testing (TORO 1 and 2) has been reported to suppress drug-resistant HIV replication more efficiently that the optimized regimen alone (17, 18).

The emergence of T-20-resistant HIV-1 was first reported in clinical patients receiving T-20 monotherapy in a phase I clinical trial (28) and subsequently in combined regimens employed in phase II and III trials of T-20 (23, 25). The T-20 susceptibility of recombinant HIV-1 containing the identified substitutions was examined in vitro and considered to be moderately resistant (5.4- to 6.3-fold) (28). However, the detailed mechanism of resistance of these variants still remains to be elucidated. On the other hand, Rimsky et al. revealed that three continuous amino acids in the N-HR (GIV at positions 36 to 38 of gp41) were crucial for the inhibition of HIV-1 entry by T-20 and for efficient association between N-HR and T-20 in vitro (26). Fikkert et al. also reported that HIV-1 variants resistant to T-20 contained substitutions in gp41, L33S and N43K, and a deletion of 5 amino acids, FNSTW (ΔFNSTW), in the V4 region of gp120 (9). L33S and N43K contributed to T-20 resistance, whereas the 5-amino-acid deletion alone had little effect on T-20 sensitivity. These results suggest that substitutions in the N-HR directly affect T-20 binding. Although the baseline sensitivity of HIV-1 to T-20 is defined by amino acid substitutions in gp41, coreceptor specificity is influenced by substitutions in the V3 loop in gp120, affects the fusion kinetics, and modulates T-20 sensitivity (4, 5).

To elucidate the mechanism of resistance to the peptide fusion inhibitors, we generated and characterized HIV-1 variants resistant to C34, a gp41 C-HR-derived peptide (2, 22) (Fig. 1A). During the selection of C34-resistant variants, we observed a 5-amino-acid deletion in the gp120 V4 region and a total of seven amino acid substitutions in gp41. Among the deletion and the substitutions, I37K and N126K play a key role in the resistance to C-HR-derived peptides, including T-20. Other deletions or substitutions were considered to enhance C34 resistance and/or improve the impaired replication kinetics. A30V and D36G maintained the Rev-responsive element (RRE) structure destabilized by I37T and I37K, respectively. Thus, these results reveal that the deletions or substitutions conferring resistance are restricted by both gp41 and RRE functions, suggesting that HIV-1 fusion is one of the most ideal targets for chemotherapy.

MATERIALS AND METHODS

Cells and viruses. MT-2 and Cos-7 cells were grown in RPMI 1640- and Dulbecco's modified Eagle medium-based culture medium, respectively. HeLa-

* Corresponding author. Mailing address: Laboratory of Virus Immunology, Institute for Virus Research, Kyoto University, 53 Shogoin Kawaramachi, Sakyoku, Kyoto 606-8507, Japan. Phone 81-75-751-3986. Fax: 81-75-751-3986. E-mail: ekodama@virus.kyoto-u.ac.jp.

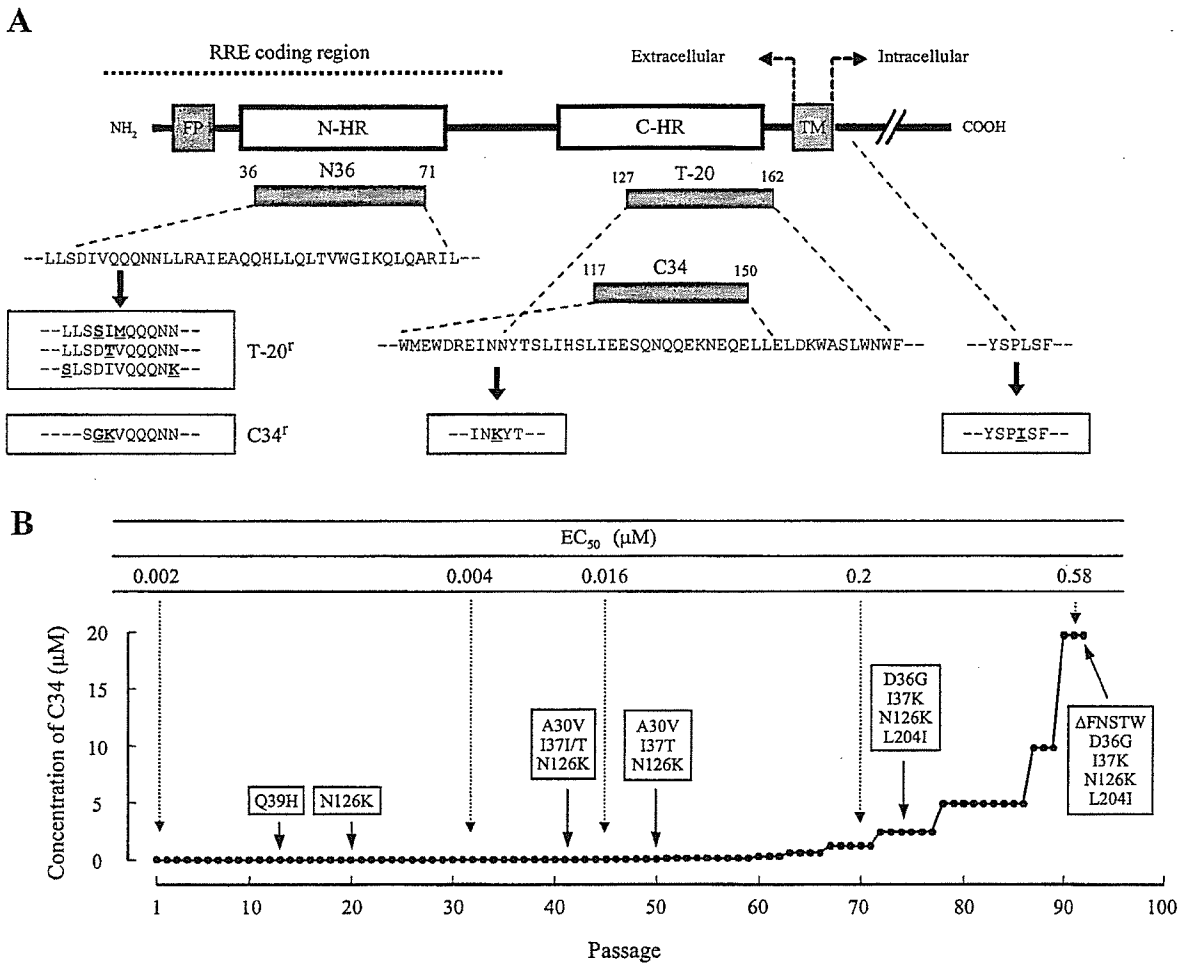

FIG. 1. Schematic view of HIV-1 gp41 (A) and induction of C34-resistant HIV-1 (B). The locations of the fusion peptide (FP), N-terminal heptad repeat region (N-HR), C-terminal heptad repeat region (C-HR), transmembrane domain (TM), various gp41-derived peptides, and the Rev-responsive element (RRE) coding region are shown (A). The residue numbers of each peptide correspond to their positions in gp41. The bold underlined letters in the boxes indicate the novel mutations that have been reported in T-20-resistant HIV-1 variants (T-20^r) in vitro (9, 26) and that have been observed in C34-resistant HIV-1 variants (C34^r). (B) HIV-1_{NL4-3} was passaged in the presence of increasing concentrations of C34 in MT-2 cells. The dose-escalating selection was carried out for a total of 93 passages, with compound concentrations ranging from 0.0001 to 20 μM. At the indicated passages, proviral DNAs from the lysates of infected cells were sequenced, and the EC_{50}s of the HIV-1 variants were determined with the MAGI assay.

CD4-LTR-β-gal cells were kindly provided by M. Emerman through the AIDS Research and Reference Reagent Program, Division of AIDS, National Institute of Allergy and Infectious Disease (Bethesda, Md.), and used for the drug susceptibility assay (multinuclear activation of galactosidase indicator [MAGI] assay) as described previously (12, 14, 21). An HIV-1 infectious clone, pNL4-3, which was kindly provided by H. Sakai, Institute for Virus Research, Kyoto University (Kyoto, Japan), was used for constructions and the production of HIV-1 variants. A wild-type HIV-1, HIV-1_{WT}, was generated by transfection of pNL4-3 into Cos-7 cells.

Antiviral agents. The peptides used were N36, derived from the N-HR of gp41, and C34 and T-20, derived from the C-HR of gp41. The peptides were synthesized as described previously (24) and are depicted in Fig. 1A. 2′,3′-Dideoxycytidine (ddC) was purchased from Sigma (St. Louis, Mo.).

Determination of drug susceptibility of HIV-1. The peptide sensitivity of infectious clones was determined by the MAGI assay with some modifications (14, 21). Briefly, the target cells (HeLa-CD4-LTR-β-gal; 10^4 cells/well) were plated in 96-well flat microtiter culture plates. On the following day, the cells were inoculated with the HIV-1 clones (60 MAGI U/well, giving 60 blue cells after 48 h of incubation) and cultured in the presence of various concentrations of drugs in fresh medium. Forty-eight hours after viral exposure, all the blue cells stained with X-Gal (5-bromo-4-chloro-3-indolyl-β-D-galactopyranoside) were counted in each well. The activity of test compounds was determined as the concentration that blocked HIV-1 replication by 50% (50% effective concentration [EC_{50}]).

Construction of recombinant HIV-1 clones. Recombinant infectious HIV-1 clones carrying various mutations in gp120 and/or gp41 were generated by using pNL4-3. Briefly, the desired mutations were introduced into the NheI-BamHI region (1,220 bp) of pSLgp41$_{WT}$, which encoded nucleotides 7250 to 8469 of pNL4-3, by an oligonucleotide-based mutagenesis method (29). NheI-BamHI fragments were inserted into pNL4-3, generating various molecular clones with the desired mutations. Each molecular clone was transfected into Cos-7 cells (10^5 cells/six-well culture plate). After 48 h, MT-2 cells (10^6 cells/well) were added and cocultured with the Cos-7 cells for an additional 24 h. When an extensive cytopathic effect (CPE) was observed, the supernatants were harvested and stored at −80°C until use.

Generation of HIV-1 variants resistant to C34. MT-2 cells were exposed to HIV-1_{WT} and cultured in the presence of C34 at an initial concentration of 0.0001 μM. Cultures were incubated at 37°C until an extensive CPE was observed. The culture supernatants were used for further passages in MT-2 cells in the presence of twofold increasing concentrations of C34 when massive CPEs

were seen in the earlier periods. Such dose-escalating culture was performed until resistant variants were obtained. This selection was carried out for a total of 93 passages. At the indicated passages (Fig. 1B), the sequence of the *env* region was determined by direct sequencing of the proviral DNA extracted from the infected MT-2 cells.

Viral replication kinetics assay. MT-2 cells (10^5 cells/5 ml) were infected with each virus preparation (500 MAGI U) for 4 h. The infected cells were then washed and cultured in a final volume of 5 ml. The culture supernatants (100 μl) were harvested on days 1, 2, 4, 6, and 8 after infection, and the p24 antigen amounts were determined.

For competitive HIV-1 replication assays (CHRA), two titrated infectious clones to be examined were mixed and added to MT-2 cells (10^5 cells/3 ml) as described previously (15) with some modifications. To ensure that the two infectious clones being compared were of approximately equal infectivity, a fixed amount (500 MAGI U) of one infectious clone was mixed with three different amounts (250, 500, and 1,000 MAGI U) of the other infectious clone. On day 1, one third of the infected MT-2 cells were harvested and washed twice with phosphate-buffered saline, and the cellular DNA was extracted. The purified DNA was subjected to nested PCR and then direct DNA sequencing. The HIV-1 coculture which best approximated a 50:50 mixture on day 1 was further propagated. Every 6 to 7 days, the cell-free supernatant of the virus coculture (1 ml) was transmitted to new uninfected MT-2 cells. The cells harvested at the end of each passage were subjected to direct sequencing, and the viral population change was determined.

Binding assay. Each peptide (40 μM) was mixed with 10 mM phosphate-buffered saline–140 mM NaCl, pH 7.4, in an Aviv model 202 DS spectrometer equipped with a thermoelectric temperature controller. The thermal stability was assessed by monitoring the change in the circular dichroism signal at 222 nm. The midpoint of the thermal unfolding transition (melting temperature [T_m]) of each complex was determined as described previously (24).

Gel shift assay. RNA of the RRE region and recombinant Rev were prepared as described previously (10) with some modifications. Briefly, the RRE region of the variants (nucleotides 7748 to 8009 of pNL4-3) was introduced into pBlue-Script (Stratagene, La Jolla, Calif.). In vitro RNA transcription was performed with T7 RNA polymerase and [^{32}P]UTP. Recombinant Rev was generated by use of the pGEX-6P-1/BL21 expression system (Amersham Biosciences, Piscataway, N.J.). The RNA and Rev were mixed at 25°C for 20 min in binding buffer (50 mM Tris-HCl, pH 7.5, 150 mM KCl, 1 mM dithiothreitol, 8% glycerol, 50 μg of tRNA/ml, and 100 μg of bovine serum albumin/ml) and subjected to native acrylamide gel electrophoresis.

RESULTS

Amino acid substitutions identified in the *env* region of C34-resistant HIV-1. At passage 14 (P-14) in the culture where HIV-1 was propagating in the presence of C34 (0.0032 μM), one amino acid substitution, glutamine to histidine at position 39 (Q39H), in the N-HR of gp41 was transiently identified (Fig. 1B). At P-20 (0.0064 μM), a substitution, N126K, was newly identified in the C-HR, whereas Q39H had returned to the original wild-type amino acid. At P-41 (0.026 μM), two substitutions, A30V and I37I/T (mixture of I and T), were observed in the N-HR in addition to N126K, while at P-50 (0.077 μM), definitive I37T was detected (A30V/I37T/N126K) (Fig. 1B). At P-75 (2.5 μM), A30V had returned to the original wild-type amino acid, D36G was detected, I37T was substituted for I37K, and L204I, which was located in the cytoplasmic domain of gp41, was identified (D36G/I37K/N126K/L204I). At P-92 (20 μM), a deletion of five amino acids, FNSTW, in the V4 loop of gp120 (ΔFNSTW) was observed together with the four substitutions (ΔFNSTW/D36G/I37K/N126K/L204I) (Fig. 1B). In addition to the *env* region, we also examined the Tat- and Rev-encoding regions but did not observe any substitutions. These results suggest that, in order to develop a higher resistance to C34, HIV-1 acquires not only multiple substitutions in gp41 but also the 5-amino-acid deletion in gp120.

Susceptibility of the different *env* recombinant viruses to fusion inhibitors. To clarify which substitutions among the identified changes were responsible for C34 resistance, we first generated infectious HIV-1 clones containing the deletion (ΔFNSTW) in gp120 or the single amino acid substitutions (A30V, D36G, I37T, I37K, Q39H, N126K, or L204I) in gp41 that were observed during the selection procedure (Fig. 1B). We also evaluated the activities of the gp41-derived peptides N36, T-20, and C34 and a reverse transcriptase inhibitor used as a control, ddC, against these strains with the MAGI assay (Table 1).

HIV-$1_{\Delta FNSTW}$, HIV-1_{A30V}, HIV-1_{Q39H}, and HIV-1_{L204I} showed weak resistance to C34 compared with HIV-1_{WT} (less than fivefold). Interestingly, D36G, observed in the majority of HIV-1 strains (16), conferred an increased T-20 susceptibility to HIV-1 (10-fold), in agreement with previous reports (20, 26), whereas D36G did not contribute C34 resistance by itself (0.8-fold). Although I37T has also been reported as one of the T-20 resistance mutations in vitro, its detailed mechanism of resistance remains unknown (20, 26). In our experiments, I37T conferred T-20 and C34 resistance to HIV-1 (13- and 11-fold, respectively), and I38K also conferred both T-20 and C34 resistance (212- and 13-fold, respectively). HIV-1_{N126K} showed moderate resistance to C34 (6.8-fold). Neither the deletion in gp120 nor any of the substitutions in gp41 conferred resistance to N36 or ddC (Table 1).

Although the I37 substitutions appeared to be primarily responsible for C34 resistance, the C34 resistance levels of the I37 substitution variants were not comparable to that of the selected virus at P-93 (EC_{50}, 0.78 μM). Therefore, we generated infectious HIV-1 clones containing the identified substitutions combined with I37T or I37K and determined their susceptibilities to the peptides (Table 1). The combination of I37K and N126K enhanced C34 resistance (13- to 28-fold), whereas HIV-1_{I37T}, HIV-$1_{I37T/N126K}$, and HIV-$1_{A30V/I37T/N126K}$ showed comparable resistance levels to C34. Moreover, I37K/N126K combined with D36G (D36G/I37K/N126K) enhanced C34 resistance (72-fold), although the L204I substitution combined with D36G/I37K/N126K decreased the levels of resistance to both T-20 and C34 (10- and 54-fold, respectively). A clone containing the deletion in gp120 and four substitutions in gp41, HIV-$1_{\Delta FNSTW/D36G/I37K/N126K/L204I}$, showed the highest resistance to C34 (83-fold) and cross-resistance to T-20 (64-fold). These results indicate that the I37K substitution is mainly responsible for C34 resistance, whereas the other substitutions enhance the resistance or improve the impaired viral replication kinetics.

Next, we generated a T-20-resistant molecular clone which had been previously reported (26), HIV-$1_{D36S/V38M}$, and evaluated the susceptibility to N36, T-20, and C34. HIV-$1_{D36S/V38M}$ showed moderate resistance to both T-20 and C34 (5.1- and 7.7-fold, respectively) (Table 1). We also generated HIV-1 variants that contained each of the single substitutions, HIV-1_{D36S} and HIV-1_{V38M}. HIV-1_{D36S} did not contribute to the resistance, although HIV-1_{V38M} showed cross-resistance to T-20 and C34 (26- and 15-fold, respectively). Combined with the finding that I37K is the major mutation for resistance to C34, this region, positions 37 and 38 of gp41, appears to be involved in resistance to both T-20 and C34, while changes at position 36 appear to be largely restricted in their effects to T-20.

TABLE 1. Antiviral activity of HIV-1 gp41-derived peptides against gp120 and/or gp41 recombinant viruses[a]

Virus or substitution	EC_{50} (nM)			
	ddC	T-20	N36	C34
$HIV\text{-}1_{WT}$[b]	264	12	51	2.1
ΔFNSTW[c]	98 (0.4)	18 (1.5)	50 (1.0)	9.5 (4.6)
A30V	205 (0.8)	6.3 (0.5)	38 (0.7)	7.0 (3.4)
D36G	173 (0.7)	0.92 (0.1)	90 (1.7)	1.6 (0.8)
D36S[e]	166 (0.6)	6.6 (0.6)	89 (1.7)	3.7 (0.6)
I37T	284 (1.1)	156 (13)	40 (0.8)	23 (11)
I37K	326 (1.2)	2,482 (212)	99 (1.9)	27 (13)
V38M[e]	223 (0.8)	305 (26)	94 (1.8)	31 (15)
Q39H[d]	330 (1.3)	1.9 (0.2)	165 (3.2)	5.3 (2.6)
N126K[d]	380 (1.4)	23 (1.9)	137 (2.7)	14 (6.8)
L204I	247 (0.9)	13 (1.1)	105 (2.0)	4.4 (2.1)
D36S/V38M[e]	294 (1.1)	60 (5.1)	46 (0.9)	16 (7.7)
I37T/N126K	292 (1.1)	158 (14)	54 (1.1)	22 (11)
I37K/N126K	309 (1.2)	1,570 (134)	51 (1.0)	57 (28)
A30V/I37K/N126K	409 (1.5)	198 (17)	119 (2.3)	22 (10)
D36G/I37K/N126K	329 (1.2)	269 (23)	156 (3.0)	148 (72)
D36G/I37K/N126K/L204I[d]	209 (0.8)	117 (10)	41 (1.2)	112 (54)
ΔFNSTW/D36G/I37K/N126K/L204I[d]	213 (0.8)	746 (64)	54 (1.0)	171 (83)

[a] Anti-HIV activity was determined with the MAGI assay. The data shown are mean values obtained from the results of at least three independent experiments, and resistance (*n*-fold) in EC_{50} for recombinant viruses compared to $HIV\text{-}1_{WT}$ is shown in parentheses.
[b] $HIV\text{-}1_{NL4\text{-}3}$ was used was a wild-type virus.
[c] ΔFNSTW is the deletion of 5 amino acids at positions 364 to 368 in the gp120 V4 region of $HIV\text{-}1_{NL4\text{-}3}$.
[d] Mutant viruses observed during induction of C34 resistance variants in vitro (Fig. 1B).
[e] D36S/V38M has been reported for T-20-resistant HIV-1 variants (26).

Peptide binding affinity. To clarify the effect of the substitutions on the interaction of N-HR and C-HR, the binding affinity of the peptides in vitro was examined with the synthesized peptides (Table 2). The affinity between $N36_{D36G/I37K}$ and C34 was unstable even at 37°C, indicating that the peptide inhibitor C34 hardly bound to $N36_{D36G/I37K}$. However, it is still unclear whether it is a direct effect of the N-HR mutations decreasing the affinity of C34 binding or an indirect effect of the N-HR mutations destabilizing the N-HR trimer formation. In contrast, $C34_{N126K}$, with the substitution responsible for the resistance, showed enhanced binding affinity not only to N36 but also to $N36_{D36G/I37K}$. Thus, there are two implications of mutations in gp41 for conferring C34 resistance: the decreased affinity of C34 for $N36_{D36G/I37K}$ and the increased affinity of $C34_{N126K}$ for both $N36_{WT}$ and $N36_{D36G/I37K}$. In other words, the D36G and I37K substitutions in the N-HR interfere with the binding of the peptide inhibitors, such as T-20 and C34, and N126K in the C-HR enhances the intra-gp41 binding of N-HR and C-HR compared with the peptide inhibitors.

Replication kinetics of C34-resistant variants. To determine the effects of the identified deletion and mutations on HIV-1 replication, we first examined the replication kinetics of HIV-1 variants by p24 production in the culture supernatants. The p24 production by the variants ranged from 14 to 34% of that of $HIV\text{-}1_{WT}$ ($HIV\text{-}1_{I37T/N126K}$, 14%; $HIV\text{-}1_{N126K}$, 30%; and $HIV\text{-}1_{A30V/I37T/N126K}$, 34%) as determined at day 8 (Fig. 2). Next, the replication levels of variants with representative substitutions were compared by CHRA. The resistances (*n*-fold) of the variants are also shown in Fig. 2. Since $HIV\text{-}1_{Q39H}$ was considered to be one of the polymorphisms and appeared only transiently, we first compared the replication of $HIV\text{-}1_{WT}$ and $HIV\text{-}1_{N126K}$ and found an impaired replication profile for $HIV\text{-}1_{N126K}$. The variant with a combination including the I37T substitution, $HIV\text{-}1_{I37T/N126K}$, which was not observed during selection, showed the slowest replication profile. To develop an $HIV\text{-}1_{A30V/I37T/N126K}$ variant, the A30V substitution was introduced first, and then the I37T substitution was introduced (Fig. 1B). This was consistent with the results of the CHRA that the replication profile of $HIV\text{-}1_{A30V/I37T/N126K}$ was

TABLE 2. Binding affinity of wild and mutated peptides[a]

Peptide	T_m (°C)
N36/C34	49.5
$N36_{D36G/I37K}$/C34	38.5
N36/$C34_{N126K}$	55.0
$N36_{D36G/I37K}$/$C34_{N126K}$	45.0

[a] The binding affinity of the peptides is shown with T_m values.

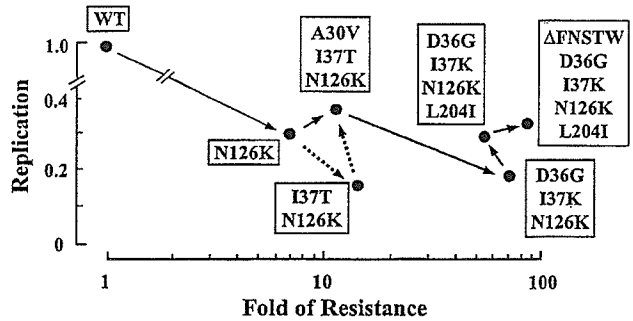

FIG. 2. Replication kinetics of the resistant variants. The replication kinetics determined by p24 antigen production and the CHRA are summarized. The data are depicted as the resistance (*x* axis) and replication (*y* axis) compared with those of $HIV\text{-}1_{WT}$. Variants observed (continuous arrows) and not observed (dashed arrows) in the selection are shown in the order of their emergence.

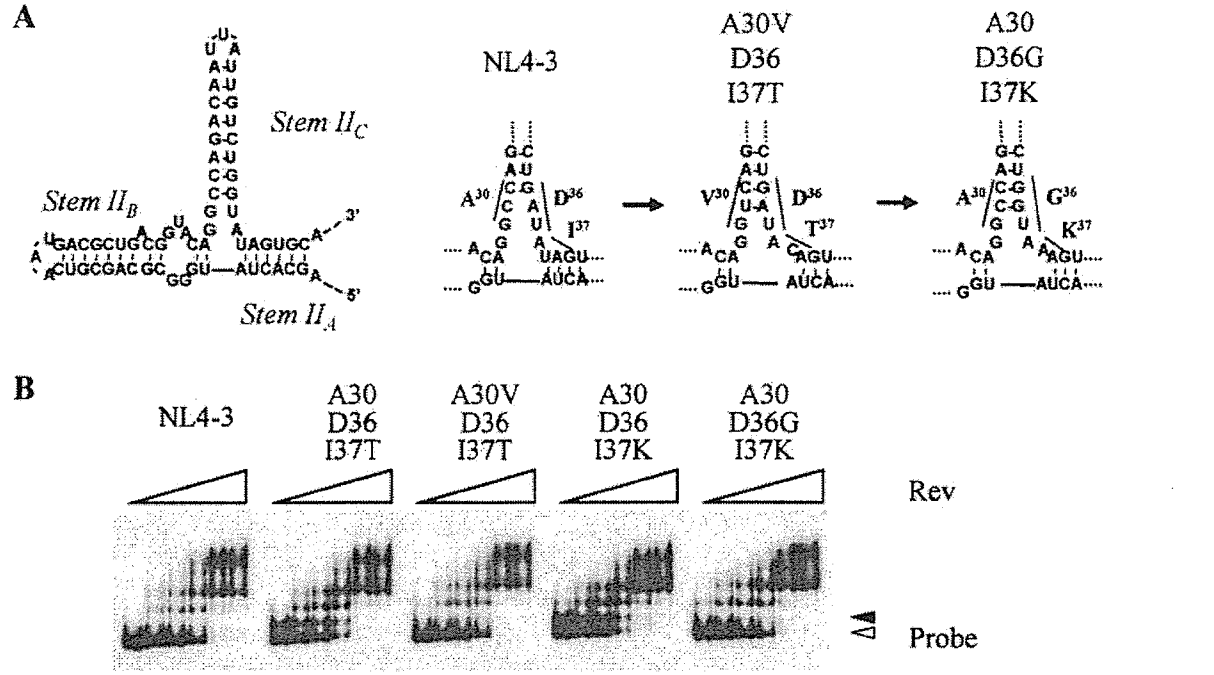

FIG. 3. Putative secondary structure of the RRE and locations of the nucleotides corresponding to the substitutions. The II_A, II_B, and II_C stems and the effects of the nucleotide substitutions are shown (A). A30V (GCC to GTC) to D36 (GAT) and A30 (GCC) to D36G (GAT to GGT) are located complementary to each other in the stem II_B (underlined). The effects of the nucleotide substitutions on the Rev-RRE interaction were examined by gel shift assays (B). The RRE of HIV-1_{I37T} and HIV-1_{I37K} displayed two signals. The amounts of Rev used were 0, 20, 40, 80, 160, 240, and 320 nM (left to right).

greater than that of HIV-$1_{I37T/N126K}$, suggesting that the A30V substitution improved the impaired replication profile of HIV-$1_{I37T/N126K}$. Since both HIV-1_{I37K} and HIV-$1_{I37K/N126K}$ could replicate for only a few passages, these variants could not be studied. For I37K/N126K substitutions, D36G instead of A30V substitution seemed to be suitable in order to maintain resistance and replication, although the replication of HIV-$1_{D36G/I37K/N126K}$ still remained impaired. The L204I substitution improved the replication kinetics of HIV-$1_{D36G/I37K/N126K}$. The deletion in the V4 region contributed to both the increased resistance and replication. These results indicate that among the deletion and the substitutions, I37T/K and N126K, and especially I37K, are related to resistance, while A30V, D36G, and L204I are associated with improvement of replication and the deletion in the V4 region had modest effects on increased resistance and replication.

Rev and RRE interactions. The nucleotides for the substitutions A30V, D36G, and I38T/K also encode the RRE, and the nucleotides for A30 and D36 are located complementary to each other in stem II_C (Fig. 3A). A30V emerged along with I37T and intact D36, and D36G was found with I37K and intact A30. Thus, these mutations were thought to maintain the positioning of stems II_A and II_B in the tertiary structure of the RRE. To examine the effect of these nucleotide substitutions on the Rev-RRE interaction, we performed a gel shift assay. The secondary structure of the RRE that contained the I37T or I37K substitutions showed two forms (Fig. 3B). Introduction of A30V, which could improve the replication of HIV-1_{I37T}, changed the two RRE structures into a structure identical to that observed in the wild type. D36G observed with I37K also changed the separated RRE structure. However, little difference (less than 10%) in the Rev binding caused by the substitutions was observed between the wild-type and the mutated RRE (Fig. 3B). These results indicate that substitutions at A30 or D36 maintain the stability of the RRE secondary structure that is affected by nucleotide substitutions at I37.

DISCUSSION

After adsorption to cells followed by conformational changes of gp120, HIV fusion takes place by interaction and binding of the N-HR and C-HR of gp41. C-HR-derived peptides, e.g., T-20 or C34, inhibit HIV replication as a decoy for C-HR (2, 30). Previous reports showed that mutations in N-HR (19) were associated with resistance to T-20 (9, 25, 26, 28). In this study, we showed that competition between C34 and C-HR also plays a key role in acquiring resistance. However, in order to develop high resistance to C34, changes in the binding affinity of N-HR, as observed in T-20 resistance, are insufficient on their own, and an additional mutation in C-HR is necessary. According to the crystal structure of gp41 (2), none of the substitutions observed in this study are located on the binding surface of the N-HR or C-HR. Even one of the primary mutations that directly contribute to the resistance, I37K, is not located on the binding surface of N-HR. We also identified a primary mutation, N126K, that is located outside of the binding surface of C-HR. Although the significance of these locations still remains to be defined at present, further structural analysis may provide insights into the mechanism of binding

enhancement. Our observations also provide evidence that small compounds interacting directly with the binding surface seem to inhibit HIV replication efficiently, since HIV would hardly be mutated on the binding surface.

During the selection of the C34-resistant variants, the substitutions were introduced in the following order: a substitution (N126K) associated with susceptibility to C34 was introduced first, followed by a substitution (A30V) associated with replication. L204I also improved the replication kinetics of HIV-$1_{D36G/I37K/N126K}$. It is likely that substitutions that are associated with resistance usually impair the replication kinetics, resulting in selection of HIV-1 variants containing substitutions that improve the replication disadvantages. This hypothesis has been proved with analyses of replication kinetics of T-20-resistant variants described previously (20). Moreover, such substitution patterns have previously been observed in multi-dideoxynucleoside-resistant variants (15, 21). However, the mechanism of replication improvement in multi-dideoxynucleoside-resistant variants remains unknown. In this study, I37 is one of the key amino acids for C34 resistance, and it is located in an important region for the Rev-RRE interaction (13). The significance of the secondary mutations, A30V and D36G, for improvement of the RRE structural stability impaired by I37T or I37K is thought to be that they maintain both gp41 and RRE functions. In contrast to the C34 resistance mutations, nucleotides encoding some T-20 resistance mutations, L33S and N43K (9), are located in a single-stranded bulge region of the stem II_C loop top (UUA to UCA) (Fig. 3A) and in the bulge region of stem III, indicating that the structural changes to the RRE would be minimal, while other T-20 resistance mutations (20), such as G36D, G36S, I37K, and possibly V38A and V38 M, appear to alter the stability of the RRE stem II_C structure and to impair the replication kinetics. To date, the Rev-RRE interaction has mainly been examined for stem II_B, since Rev directly binds to it (10, 13). Although the functions of stems II_A and II_C remain to be defined, it is possible that the secondary mutations in stem II_C influence the Rev-RRE interaction, since we have shown that the secondary mutations were introduced simultaneously with the primary mutations and improved replication. These results also indicate that the conformation of the RRE is essential for the Rev-RRE interaction and not just the nucleotide sequence of the RRE itself.

NL4-3 gp41 contains four N-glycan attachment sites, N-X-S/T, located at N100-A-S, N105-K-S, N114-M-T, and N126-Y-T. These four sites are highly conserved in various HIV strains (11, 16). Mutational analysis revealed that each substitution of the N glycosylation sites had a modest effect on HIV replication, whereas some combined substitutions severely impaired replication (11). Although the effect of N126-glycan on binding of the N-HR and C-HR remains unknown, it would be possible that N126-glycan plays some roles for C34 resistance. Different effects of N126K substitution on susceptibility to T-20 and C34 (1.9- and 6.8-fold, respectively) were observed (Table 1). This result might be accounted for by the finding that N126 locates at −1 (outside) from the N terminus of T-20, whereas it locates inside (+10) of C34 (Fig. 1A).

It has been reported that a tyrosine-based sorting signal in the gp41 cytoplasmic domain, Y201-X-X-L, was involved in trafficking and targeting to the plasma membrane of the gp41 (3). The motif is highly conserved among various HIV strains (16, 19). Although the role of Y201 for infectivity has been studied in detail (3, 19), that of L204 remains to be defined. In the present study, we showed that the L204I substitution enhanced viral replication, suggesting that L204, as well as Y201, plays an important role for viral replication.

pNL4-3 was established as a molecular clone of wild-type HIV-1 (1) and is widely used in HIV research. However, it represents only one of the wild-type HIV-1 variants. In fact, even in the absence of C34, we still observed several substitutions in NL4-3 that were identified in the C34 selection, e.g., A30V and Q39H. These substitutions are also observed in some treatment-naïve clinical isolates (16). It is well known that HIV reverse transcriptase makes several nucleotides miss incorporation during the reverse transcription, suggesting that each HIV isolate, even in the wild-type population, contains several substitutions in the integrated DNA genome. D36 is identified only in pNL4-3-derived clones, although the G36/I37/V38 motif is well conserved, not only in HIV-1 but also in HIV-2 and simian immunodeficiency virus strains (16). Furthermore, the 5-amino-acid deletion in gp120 was reported not only in a fusion inhibitor, T-20 (9), but also in CD4-gp120-binding inhibitors DS5000 (8) and AR177 (Zintevir) (7), CXCR4 antagonists, bicyclams JM2763 and SID791 (6), and SDF-1α-resistant variants (27). In these reports, pNL4-3-derived viruses were also used for the selection of the resistant variants. Only pNL4-3 has the 5-amino-acid tandem sequence FNSTWFNSTW in the gp120 V4 region. Therefore, this deletion is thought to be specific for HIV-1_{NL4-3}, although the 5-amino-acid deletion conferred weak C34 resistance. These results indicate that we should be careful before concluding that such substitutions are involved in the resistance or replication kinetics.

In conclusion, HIV acquires resistance against C34 by mutations in both N-HR and C-HR. However, mutations in N-HR are restricted by Rev-RRE and/or gp120-gp41 interactions, suggesting that HIV-1 fusion is one of the most attractive targets for blocking HIV infection.

ACKNOWLEDGMENTS

We thank Hiroaki Mitsuya for helpful suggestions and Ayako Yoshioka for manuscript preparation.

This work was supported in part by a grant for the Promotion of AIDS Research from the Ministry of Health and Welfare of Japan (M.M.), a grant for Research for Health Sciences Focusing on Drug Innovation from the Japan Health Sciences Foundation (E.K.), and a grant from the Ministry of Education, Culture, Sports, Science, and Technology of Japan (E.K.). D.N. is supported by the 21st Century COE Program of the Ministry of Education, Culture, Sports, Science, and Technology.

REFERENCES

1. **Adachi, A., H. E. Gendelman, S. Koenig, T. Folks, R. Willey, A. Rabson, and M. A. Martin.** 1986. Production of the acquired immunodeficiency syndrome-associated retrovirus in human and nonhuman cells transfected with an infectious molecular clone. J. Virol. **59**:284–291.
2. **Chan, D. C., D. Fass, J. M. Berger, and P. S. Kim.** 1997. Core structure of gp41 from the HIV envelope glycoprotein. Cell **89**:263–273.
3. **Day, J. R., C. Munk, and J. C. Guatelli.** 2004. The membrane-proximal tyosine-based sorting signal of human immunodeficiency virus type 1 gp41 is required for optimal viral infectivity. J. Virol. **78**:1069–1079.
4. **Derdeyn, C. A., J. M. Decker, J. N. Sfakianos, X. Wu, W. A. O'Brien, L. Ratner, J. C. Kappes, G. M. Shaw, and E. Hunter.** 2000. Sensitivity of human immunodeficiency virus type 1 to the fusion inhibitor T-20 is modulated by coreceptor specificity defined by the V3 loop of gp120. J. Virol. **74**:8358–8367.

5. **Derdeyn, C. A., J. M. Decker, J. N. Sfakianos, Z. Zhang, W. A. O'Brien, L. Ratner, G. M. Shaw, and E. Hunter.** 2001. Sensitivity of human immunodeficiency virus type 1 to fusion inhibitors targeted to the gp41 first heptad repeat involves distinct regions of gp41 and is consistently modulated by gp120 interactions with the coreceptor. J. Virol. **75**:8605–8614.
6. **De Vreese, K., V. Kofler-Mongold, C. Leutgeb, V. Weber, K. Vermeire, S. Schacht, J. Anne, E. De Clercq, R. Datema, and G. Werner.** 1996. The molecular target of bicyclams, potent inhibitors of human immunodeficiency virus replication. J. Virol. **70**:689–696.
7. **Este, J. A., C. Cabrera, D. Schols, P. Cherepanov, A. Gutierrez, M. Witvrouw, C. Pannecouque, Z. Debyser, R. F. Rando, B. Clotet, J. Desmyter, and E. De Clercq.** 1998. Human immunodeficiency virus glycoprotein gp120 as the primary target for the antiviral action of AR177 (Zintevir). Mol. Pharmacol. **53**:340–345.
8. **Este, J. A., D. Schols, K. De Vreese, K. Van Laethem, A. M. Vandamme, J. Desmyter, and E. De Clercq.** 1997. Development of resistance of human immunodeficiency virus type 1 to dextran sulfate associated with the emergence of specific mutations in the envelope gp120 glycoprotein. Mol. Pharmacol. **52**:98–104.
9. **Fikkert, V., P. Cherepanov, K. Van Laethem, A. Hantson, B. Van Remoortel, C. Pannecouque, E. De Clercq, Z. Debyser, A.-M. Vandamme, and M. Witvrouw.** 2002. *env* chimeric virus technology for evaluating human immunodeficiency virus susceptibility to entry inhibitors. Antimicrob. Agents Chemother. **46**:3954–3962.
10. **Henderson, B. R.** 1997. Interaction between HIV Rev and nuclear import and export factors: the Rev nuclear localisation signal mediates specific binding to human importin-β. J. Mol. Biol. **274**:693–707.
11. **Johnson, W. E., J. M. Sauvron, and R. C. Desrosiers.** 2001. Conserved, N-linked carbohydrates of human immunodeficiency virus type 1 gp41 are largely dispensable for viral replication. J. Virol. **75**:11426–11436.
12. **Kimpton, J., and M. Emerman.** 1992. Detection of replication-competent and pseudotyped human immunodeficiency virus with a sensitive cell line on the basis of activation of an integrated β-galactosidase gene. J. Virol. **66**: 2232–2239.
13. **Kjems, J., M. Brown, D. D. Chang, and P. A. Sharp.** 1991. Structural analysis of the interaction between the human immunodeficiency virus Rev protein and the Rev response element. Proc. Natl. Acad. Sci. USA **88**:683–687.
14. **Kodama, E. I., S. Kohgo, K. Kitano, H. Machida, H. Gatanaga, S. Shigeta, M. Matsuoka, H. Ohrui, and H. Mitsuya.** 2001. 4′-Ethynyl nucleoside analogs: potent inhibitors of multidrug-resistant human immunodeficiency virus variants in vitro. Antimicrob. Agents Chemother. **45**:1539–1546.
15. **Kosalaraksa, P., M. F. Kavlick, V. Maroun, R. Le, and H. Mitsuya.** 1999. Comparative fitness of multi-dideoxynucleoside-resistant human immunodeficiency virus type 1 (HIV-1) in an in vitro competitive HIV-1 replication assay. J. Virol. **73**:5356–5363.
16. **Kuiken, C., B. Foley, B. Hahn, P. Marx, F. McCutchan, J. Mellors, S. Wolinsky, and B. Korber (ed.).** 2001. HIV sequence compendium 2001. Theoretical Biology and Biophysics Group, Los Alamos National Laboratory, Los Alamos, N.M.
17. **Lalezari, J. P., K. Henry, M. O'Hearn, J. S. Montaner, P. J. Piliero, B. Trottier, S. Walmsley, C. Cohen, D. R. Kuritzkes, J. J. Eron, Jr., J. Chung, R. DeMasi, L. Donatacci, C. Drobnes, J. Delehanty, and M. Salgo.** 2003. Enfuvirtide, an HIV-1 fusion inhibitor, for drug-resistant HIV infection in North and South America. N. Engl. J. Med. **348**:2175–2185.
18. **Lazzarin, A., B. Clotet, D. Cooper, J. Reynes, K. Arasteh, M. Nelson, C. Katlama, H. J. Stellbrink, J. F. Delfraissy, J. Lange, L. Huson, R. DeMasi, C. Wat, J. Delehanty, C. Drobnes, and M. Salgo.** 2003. Efficacy of enfuvirtide in patients infected with drug-resistant HIV-1 in Europe and Australia. N. Engl. J. Med. **348**:2186–2195.
19. **Lodge, R., J.-P. Lalonde, G. Lemay, and E. A. Cohen.** 1997. The membrane-proximal intracytoplasmic tyrosine residue of HIV-1 envelope glycoprotein is critical for basolateral targeting of viral budding in MDCK cells. EMBO J. **16**:695–705.
20. **Lu, J., P. Sista, F. Giguel, M. Greenberg, and D. Kuritzkes.** 2004. Relative replicative fitness of human immunodeficiency virus type 1 mutants resistant to enfuvirtide (T-20). J. Virol. **78**:4628–4637.
21. **Maeda, Y., D. J. Venzon, and H. Mitsuya.** 1998. Altered drug sensitivity, fitness, and evolution of human immunodeficiency virus type 1 with pol gene mutations conferring multi-dideoxynucleoside resistance. J. Infect. Dis. **177**: 1207–1213.
22. **Malashkevich, V. N., D. C. Chan, C. T. Chutkowski, and P. S. Kim.** 1998. Crystal structure of the simian immunodeficiency virus (SIV) gp41 core: conserved helical interactions underlie the broad inhibitory activity of gp41 peptides. Proc. Natl. Acad. Sci. USA **95**:9134–9139.
23. **Matthews, T., M. Salgo, M. Greenberg, J. Chung, R. DeMasi, and D. Bolognesi.** 2004. Enfuvirtide: the first therapy to inhibit the entry of HIV-1 into host CD4 lymphocytes. Nat. Rev. Drug Discov. **3**:215–225.
24. **Otaka, A., M. Nakamura, D. Nameki, E. Kodama, S. Uchiyama, S. Nakamura, H. Nakano, H. Tamamura, Y. Kobayashi, M. Matsuoka, and N. Fujii.** 2002. Remodeling of gp41-C34 peptide leads to highly effective inhibitors of the fusion of HIV-1 with target cells. Angew. Chem. Int. Ed. Engl. **41**:2937–2940.
25. **Poveda, E., B. Rodes, C. Toro, L. Martin-Carbonero, J. Gonzalez-Lahoz, and V. Soriano.** 2002. Evolution of the gp41 env region in HIV-infected patients receiving T-20, a fusion inhibitor. AIDS **16**:1959–1961.
26. **Rimsky, L. T., D. C. Shugars, and T. J. Matthews.** 1998. Determinants of human immunodeficiency virus type 1 resistance to gp41-derived inhibitory peptides. J. Virol. **72**:986–993.
27. **Schols, D., J. A. Este, C. Cabrera, and E. De Clercq.** 1998. T-cell-line-tropic human immunodeficiency virus type 1 that is made resistant to stromal cell-derived factor 1α contains mutations in the envelope gp120 but does not show a switch in coreceptor use. J. Virol. **72**:4032–4037.
28. **Wei, X., J. M. Decker, H. Liu, Z. Zhang, R. B. Arani, J. M. Kilby, M. S. Saag, X. Wu, G. M. Shaw, and J. C. Kappes.** 2002. Emergence of resistant human immunodeficiency virus type 1 in patients receiving fusion inhibitor (T-20) monotherapy. Antimicrob. Agents Chemother. **46**:1896–1905.
29. **Weiner, M. P., G. L. Costa, W. Schoettlin, J. Cline, E. Mathur, and J. C. Bauer.** 1994. Site-directed mutagenesis of double-stranded DNA by the polymerase chain reaction. Gene **151**:119–123.
30. **Wild, C., T. Oas, C. McDanal, D. Bolognesi, and T. Matthews.** 1992. A synthetic peptide inhibitor of human immunodeficiency virus replication: correlation between solution structure and viral inhibition. Proc. Natl. Acad. Sci. USA **89**:10537–10541.

Halogenated Thymidine Analogues Restore the Expression of Silenced Genes without Demethylation

Jun Fan,[1] Ei-ichi Kodama,[1] Yasuhiro Koh,[2] Mitsuyoshi Nakao,[3] and Masao Matsuoka[1]

[1]Laboratory of Virus Immunology, Institute for Virus Research, Kyoto University, Kyoto, Japan; [2]Department of Hematology, Kumamoto University School of Medicine; and [3]Department of Regeneration Medicine, Institute of Molecular Embryology and Genetics, Kumamoto University, Kumamoto, Japan

Abstract

Transcriptional silencing of tumor suppressor genes by aberrant DNA methylation is a characteristic frequently observed in cancer cells. Therefore, reversing this process is a therapeutic target against cancer. In this study, we established a screening system for silencing inhibitors with cell lines transfected by a retroviral vector containing a luciferase gene. More than 100 nucleosides were tested for antisilencing activity with a selected clone in which the silenced expression of luciferase could be recovered by 5-aza-2′-deoxycytidine. A group of halogenated thymidine analogues was found to reactivate transcription of not only the reporter retrovirus vector but also endogenous *glutathione-S-transferase 1* gene, without influence to DNA hypermethylation. Gel mobility shift assay showed that 5-bromo-2′-deoxyuridine (BrdUrd) or 5-iodo-2′-deoxyuridine incorporation did not affect the binding of the methyl-CpG binding protein motif to methylated DNA. Finally, in the retroviral promoter, BrdUrd treatment increased the acetylated histone H3 level and decreased methylation of histone H3 Lys^9 in accordance with recovered transcription. This study shows that halogenated thymidines have an antisilencing effect without changing DNA methylation status by interfering with step(s) between DNA methylation and histone acetylation. (Cancer Res 2005; 65(15): 6927-33)

Introduction

CpG methylation, which is established and maintained by DNA methyltransferases, is a common modification in vertebrate genome and is associated with development, differentiation, and transcriptional suppression (1). Aberrant DNA methylation in the promoter region and the subsequent silencing of tumor suppressor genes is frequently observed in various tumors, indicating that DNA methylation plays an important role in tumorigenesis (2–5). Such epigenetic changes in tumors suggest the idea that reversing aberrant hypermethylation and reactivating abnormally silenced tumor suppressor genes should be effective against tumors; this has now been designated as epigenetic therapy (5). Methylation inhibitors, which demethylate and reactivate silenced tumor suppressor genes, have shown their antitumor effects both experimentally and clinically (6). Evidence from either knockout mice or siRNA-based knockdown experiments have shown that a defect in methyl-CpG binding protein 2 (MBD2), a member of the methyl-CpG binding domain proteins that specifically bind with methylated DNA (1, 7), protected tumor-prone mice from developing tumors (8, 9). This observation implies that processes downstream of DNA methylation toward gene silencing could also be good targets for epigenetic therapy.

5-Aza-2′-deoxycytidine (5-aza-dC), first synthesized in 1964, is one of the best known methylation inhibitors (10). 5-Aza-dC is a potent inhibitor of DNA methyltransferases, and is incorporated into DNA by substituting physiologic deoxycytidine during DNA replication and functions by forming covalent complexes with DNA methyltransferases (5). To date, 5-aza-dC has been shown to be clinically effective in treatment of several human tumors (6, 11). Some other nucleoside analogues with demethylation activity have also been developed, including azacytidine, fazarabine, DHAC, and MG98 (12). More recently, another nucleoside analogue, zebularine, that demethylates and reactivates the silenced genes, was identified. Although the mechanism of zebularine is similar to that of 5-aza-dC (13), a characteristic of zebularine is that it can be p.o. administered because of its stability in an aqueous solution (14). In addition, the sequential treatment with 5-aza-dC followed by zebularine has been shown to prevent remethylation, a common obstacle in antimethylation treatments (15).

In this study, we established a screening system for compounds with antisilencing activity using a Moloney murine leukemia virus (MLV)–based retroviral vector, and identified a group of halogenated thymidine analogues that could recover gene expression without influence on DNA methylation.

Materials and Methods

Retroviral vector construction and viral particle production. The MLV-based retroviral vector, pRCV, was constructed by replacement of the neomycin phosphotransferase gene and the SV40 promoter of pLNSX with an oligonucleotide containing a multicloning site. A DNA fragment that has a luciferase gene connected with a neomycin phosphotransferase gene by an internal ribosomal entry site (IRES) was inserted into the blunted *Hin*dIII site in pRCV, yielding the retroviral vector pRCV/LIG (Fig. 1A).

The recombinant viral particles were produced by cotransfection of equal amounts of pRCV/LIG plasmids and pcDNA-VSV-G (generous gift from Hiroyuki Miyoshi, RIKEN, Tsukuba, Japan), which encodes vesicular stomatitis virus envelope glycoprotein, into a *gag-pol*–expressing packaging cell line, GP293 (Clontech, Palo Alto, CA) using Fugene reagent (Roche, Indianapolis, IN). Culture supernatants were harvested, aliquoted 48 hours later, and then stored at −80°C.

Cell culture and compounds. A human myeloid leukemia cell line, K562, was grown in RPMI 1640 (Sigma-Aldrich, St. Louis, MO) supplemented with 10% fetal bovine serum (FBS), 100 units/mL penicillin, 100 μg/mL streptomycin, and 2 mmol/L L-glutamine at 37°C under a 5% CO_2 atmosphere. The human breast cancer cell line MCF7 was grown in DMEM (Sigma) supplemented with 10% FBS, 100 units/mL penicillin, 100 μg/mL streptomycin, and 2 mmol/L L-glutamine.

Requests for reprints: Masao Matsuoka, Laboratory of Virus Immunology, Institute for Virus Research, Kyoto University, 53 Shogoin Kawahara-cho, Sakyo-ku, Kyoto 606-8507, Japan. Phone: 81-75-751-4048; Fax: 81-75-751-4049; E-mail: mmatsuok@virus.kyoto-u.ac.jp.

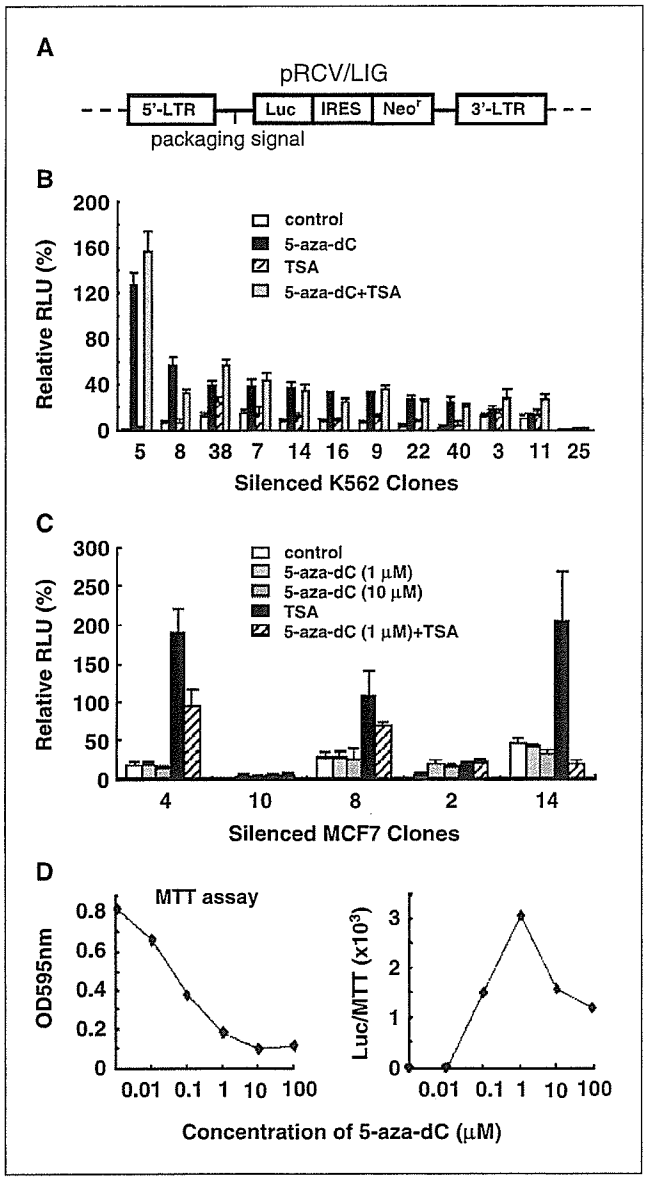

Figure 1. Establishment of a compound screening system. *A*, schematic diagram of the retroviral vector pRCV/LIG used to establish a compound screening system. *B* and *C*, response of silenced clones to 5-aza-dC and/or TSA. Silenced K562 (*B*) or MCF7 (*C*) clones were treated with 5-aza-dC for 3 days or 0.4 μmol/L TSA for 1 day, or 5-aza-dC for 2 days followed by a combination of 5-aza-dC and 0.4 μmol/L TSA for a further 1 day. The dose of 5-aza-dC used for K562 cells was 1 μmol/L. Single-tube luciferase assay was done after drug treatment. Results are described as relative light units (*RLU*) relative to the positive line of each clone. *Columns*, mean from three independent luciferase assays; *bars*, SD. *D*, optimized compound screening system tested with 5-aza-dC. On a 96-well plate, 10^3 K5 cells were exposed to graded concentrations of 5-aza-dC in a total volume of 100 μL for 5 days followed by MTT assay (*left*) or 96-well luciferase assay. Luciferase activities were normalized to the MTT values of corresponding wells and plotted against drug concentration (*right*).

5-Aza-dC, 5-azacytidine (5-aza-C), 5-bromo-2′-deoxyuridine (BrdUrd), 5-chloro-2′-deoxyuridine (CldU), 5-chloro-2′-doxycytidine (CldC), 5-iodo-2′-deoxyuridine (IdU), and trichostatin A (TSA) were purchased from Sigma.

Establishment of clones with a reporter gene. K562 and MCF7 cells were infected with the virus stock for 48 hours in the presence of 8 μg/mL polybrene. Forty-eight hours later, G418 (Nacalai Tesuque, Kyoto, Japan) was added for positive selection (0.4 mg/mL for K562 and 0.8 mg/mL for MCF7). After selection with G418 (~2 weeks), transfected clones were isolated by limiting dilution. Then, each clone was cultured under two conditions; one was cultured in medium with G418 (selection medium) and the other one in medium without G418 (nonselection medium).

Luciferase assays. Two systems, single-tube luciferase assay and 96-well plate luciferase assay, were used in this study. Single-tube luciferase assay was carried out using Luciferase Assay System (Promega, Madison, WI) according to the manufacturer's protocol. Briefly, 2×10^5 cells were collected and lysed, and then luciferase activity was detected by mixing the cell lysate and luciferase assay reagent in a luminometer tube and measured with a LB 9507 luminometer (Berthold, Bad Wildbad, Germany). For the 96-well plate luciferase assay, the Steady-Glo Luciferase Assay System (Promega) was used. Steady-Glo Reagent (100 μL) was added directly to cells growing in 100 μL of medium on a 96-well plate. Luciferase activity was measured using a Wallac 1450 MicroBeta Jet Luminometer (Perkin-Elmer, Wellesley, MA). In this study, 3-(4,5-dimethylthiazol-2-yl)-2,5-diphenyltetrazolium bromide (MTT) assay was also done to normalize the results of luciferase assay as described previously (16).

Synergistic effects of compounds. Dose-effect assays were done as reported (17). Briefly, cells were seeded onto 96-well plates and exposed to serial dilutions of each compound individually and concomitantly to both 5-aza-dC and BrdUrd or CldU at a fixed ratio (a ratio of 5-aza-dC to BrdUrd or CldU is 1:100) of doses for 3 days followed by 96-well plate luciferase assay. Doses used for 5-aza-dC were 0.05, 0.1, 0.2, 0.4, and 0.8 μmol/L; doses used for BrdUrd or CldU were 5, 10, 20, 40, and 80 μmol/L. A combination index (CI) value was calculated by the computer-based software Calcusyn developed by Chou et al. (18).

Bisulfite genomic sequencing. Sodium bisulfite treatment of genomic DNA was done as described previously (19). DNA regions were amplified using bisulfite-treated genomic DNA by nested PCR. To amplify 5′-long terminal repeat (5′-LTR) promoter region of RCV/LIG, primers used in the first PCR were 5′-TAGGATATTTGTGGTAAGTAGTTTTTGTT-3′ and 5′-CATAACATCAAACATAAACACTAAACAATC-3′. Primers for the second PCR were 5′-GGTTTAGGGTTAAGAATAGATGGTTTTTAG-3′ and 5′-CACAAATAAATTACTAACCAACTTACCTCC-3′. Primer sets target the promoter region of glutathione-S-transferase 1 (*GSTP1*) gene were as follows: For first PCR, the primer set was: 5′-TGAGAGGTGGAGGTTGTAGT-3′ and 5′-TCCTAAATCCCCTAAACCCC-3′. Primer sets used in second PCR were 5′-TGTGAAG(T/C)GGGTGTGTAAGT-3′ and 5′-CTAAAAACTCTAAACCCCATCC-3′. PCR products were purified, cloned into pGEM-T Easy vector (Promega), and sequenced using the ABI PRISM DyeDeoxy terminator cycle sequencing kit (Applied Biosystems, Foster City, CA).

Quantitative real-time reverse transcription-PCR. Total RNA was isolated from MCF7 cells using Trizol reagent (Invitrogen, Carlsbad, CA). RNA was treated with DNase I (Invitrogen) to eliminate the genomic DNA. Reverse transcription was done using random hexamer and SuperScript III reverse transcriptase (Invitrogen). cDNA product was analyzed by real-time PCR using the Taqman Universal PCR Master Mix and ABI Prism 7700 (PE Applied Biosystems, Foster City, CA) sequence detector according to the manufacturer's instruction. Specific primers and Taqman probes for *GSTP1* gene and for 18S internal control gene were used as described previously (20). PCRs were carried out in triplicate. Data was analyzed by comparative C_t method according to manufacturer's protocols (PE Applied Biosystems). The lowest detectable *GSTP1* expression that has been induced in MCF7 cells after compound treatment was set arbitrarily as 1.0, as untreated MCF7 cells are null for *GSTP1* gene expression.

Quantitative chromatin immunoprecipitation assay. Chromatin immunoprecipitation (ChIP) assay was done according to the protocol recommended by Upstate Biotechnology (Lake Placid, NY). Cells (1.5×10^6) were fixed with 1% formaldehyde for 10 minutes at room temperature, washed twice with ice-cold PBS, treated with SDS-lysis buffer [1% SDS, 50 mmol/L EDTA and 200 mmol/L Tris-HCl] for 10 minutes on ice and then sonicated. Thereafter, the DNA/protein complexes were immunoprecipitated with antibodies specific for acetylated-Histone H3 or anti-dimethyl-Histone H3 (Lys^9) antibodies (Upstate Biotechnology) overnight at 4°C. Immune complexes were collected with salmon sperm DNA-protein A and G Sepharose slurry, washed, and eluted with freshly prepared elution buffer

(1% SDS, 100 mmol/L $NaHCO_3$). Protein-DNA complexes were de-cross-linked at 65°C for 4 hours. DNA was purified and subjected to real-time PCR amplification.

ChIP DNA samples were quantified by Taqman real-time PCR assay according to the method described by Mutskov et al. (21). Briefly, primers and TaqMan probe were designed to specifically target the RCV 5′-LTR retroviral promoter. Sequences for the primer set were 5′-CCTGTGCCTTATTTGAACTA-3′ and 5′-TCTCCAAATCCCGGACG-3′. Sequence for the FAM-labeled TaqMan probe was 5′-CAGTTCGCTTCTCGCTTCTGTTCGCGC-3′. Individual PCRs were done in triplicate to control for PCR variation and mean C_t values were collected. Fold difference of the antibody bound fraction (*IP*) versus a fixed amount of input (*In*) was calculated as

$$IP/In = 2^{-\Delta\Delta C_t} = 2^{-(C_t(IP)-C_t(In))}.$$

Then, the fold difference value for a target antibody (t) was subtracted by the nonspecific value derived from rabbit IgG (t_0):

$$(IP/In)^t - (IP/In)^{t_0}.$$

Finally, the fold difference value from the positive control cell line (K5/+) was arbitrarily set as 1.0 and relative abundance of the analyzed protein from untreated or compound treated K5/− cells was subsequently calculated.

Purification of recombinant proteins used in gel mobility shift assay. Vectors that express the GST-tagged methyl-CpG binding domain of MBD1 [pGEX-2TH-MBD (1-84 amino acids)] or only GST (pGEX-2TH) as control were constructed as described previously (22). *Escherichia coli* BL21 with expression vectors were cultured overnight at 20°C, and then expression of recombinant proteins was induced by isopropyl-β-D-thiogalactopyranoside (a final concentration of 0.4 mmol/L), following further 6-hour incubation. Cells were harvested and resuspended in ice-cold PBS followed by sonication. Recombinant proteins were purified with ReadiPack GST Purification Modules (Amersham, Buckinghamshire, England), aliquoted into small fractions and stored at −20°C.

Gel mobility shift assay. Probes for mobility shift assay are shown in Fig. 5*A*. Probes (20 fmol) labeled with [γ-^{32}P]dATP were mixed with 0.4 μg purified recombinant protein in EMSA binding buffer [10 mmol/L Tris-HCl (pH 8.0), 3 mmol/L $MgCl_2$, 50 mmol/L NaCl, 0.1 mmol/L EDTA, 0.1% NP40, 2 mmol/L DTT, 5% glycerol, and 0.4 mg/mL bovine serum albumin; ref. 23] at room temperature for 30 minutes. For the competition assay, unlabeled probe DNA was added into the reaction mixture at a concentration of 10, 100, or 1,000 fold relative to the [γ-^{32}P]dATP-labeled probe. The reaction mixture (3 μL) was loaded on 8% polyacrylamide gel and run in 0.5× Tris-borate EDTA buffer. Gel was dried and exposed to Medical X-ray film (Kodak, Rochester, NY) overnight at −80°C.

Results

Establishment of a screening system for compounds with antisilencing activity. To establish a screening system for compounds with antisilencing activity, we used an MLV-based retroviral vector to monitor the silencing and recovery of reporter gene expression (24). For this purpose, an MLV-based retroviral vector pRCV/LIG was constructed, which carried a luciferase reporter cassette under the control of the retroviral 5′-LTR promoter (Fig. 1*A*). A neomycin-resistant gene was included in this vector for positive selection of transduced cells. K562 and MCF7 cell lines were infected with recombinant RCV/LIG, subcloned in the presence of G418, and tested for luciferase expression by single-tube luciferase assay. Each clone with detectable luciferase activity was cultured in the presence (positive) or the absence of G418 (negative). Luciferase activity could be maintained in cells cultured with G418, so these cells could be used as a control when the degree of silencing was judged in "negative" cells.

Time-dependent diminishing of luciferase activity was observed at various rates and degrees among the different clones after the removal of G418. Cells with a luciferase activity lower than 30% relative to their "positive" counterpart were arbitrarily considered as being silenced. Then, the silenced clones were tested about responsiveness to 5-aza-dC and TSA, an inhibitor of histone deacetylases (HDAC; Fig. 1*B* and *C*; ref. 25). Among isolated clones, the clone 5 derived from K562 (K5) showed the most prominent responsiveness to 5-aza-dC (Fig. 1*B*), whereas it did not respond to TSA. The 5′-LTR promoter region in this clone was hypermethylated although it was demethylated after exposure to 5-aza-dC (see below), indicating that promoter hypermethylation was directly associated with silencing in K5 cells. Therefore, we selected this clone for further analyses to identify antisilencing compounds. To establish a screening system with K5 cells, data from 96-well luciferase assay was normalized by values from MTT assay as parameters of the cell number (Fig. 1*D*).

On the other hand, MCF7 clones with a silenced luciferase gene could not respond to 5-aza-dC, but expressed luciferase after treatment by TSA (Fig. 1*C*). Among these clones, 5′-LTR was not methylated, indicating that silencing of the reporter gene promoter in MCF7 cells was not associated with DNA methylation (data not shown).

Halogenated thymidine analogues exhibit antisilencing activity. With this system, we screened >100 ribonucleoside analogues provided by Yamasa Corporation (Choshi, Japan) or purchased from Sigma, and identified a group of halogenated thymidines that could reactivate the transcription of luciferase gene in K5 cells (Fig. 2*A* and *B*). The identified thymidines were similar in their chemical structures (i.e., halogenated at position 5 of the pyrimidine ring; Fig. 2*A*). Among identified compounds, the effect of BrdUrd and CldU was prominent (Fig. 2*B*). In addition to thymidine analogues, CldC also showed antisilencing activity. Because CldC showed a weak antisilencing activity, it is possible that CldC is deaminated, resulting in incorporation into DNA as CldU. On the other hand, it was shown that this system successfully evaluated the antisilencing activities of the two control compounds, 5-aza-dC and 5-aza-C (Fig. 2*B*), indicating that our system was applicable for screening of antisilencing compounds.

By performing single-tube luciferase assay, we confirmed that these compounds reactivated the silenced retroviral promoter in K5 cells in a dose-dependent manner (Fig. 2*C*). Halogenated deoxyuridines substitute thymidine during incorporating into DNA, whereas 5-aza-dC is incorporated instead of deoxycytidine. Therefore, we concurrently exposed K5 cells to 5-aza-dC and either BrdUrd or CldU in various ratios and found that these compounds significantly enhanced the effect of each other (Fig. 2*C*). Luciferase activity peaked when a suboptimal dose of 5-aza-dC was paired with a high dose of BrdUrd or CldU (data not shown). Dose effect analysis was done using the method developed by Chou and Talalay (17), showing that combinations of 5-aza-dC and either BrdUrd or CldU exhibited strong synergism with the CI value decreasing dose dependently (Fig. 2*D*). These findings suggested that halogenated thymidines and 5-aza-dC exerted their antisilencing effects by different mechanisms.

Effect of 5-bromo-2′-deoxyuridine on the expression of silenced endogenous genes. Because halogenated thymidines showed antisilencing activity on hypermethylated reporter gene, we analyzed the antisilencing activity of BrdUrd on endogenous genes that are silenced through promoter DNA methylation. It has been reported that endogenous *GSTP1* gene is silenced in breast

cancer cells by DNA methylation (26). As shown in Fig. 3, BrdUrd restored *GSTP1* gene expression in a dose-dependent manner. The combination of BrdUrd and 5-aza-dC significantly increased the expression level of this gene. These results showed that BrdUrd could reactivate the silenced transcription of not only retroviral promoter in K5 cells, but also endogenous *GSTP1* gene in MCF7 cells that has been silenced by DNA methylation.

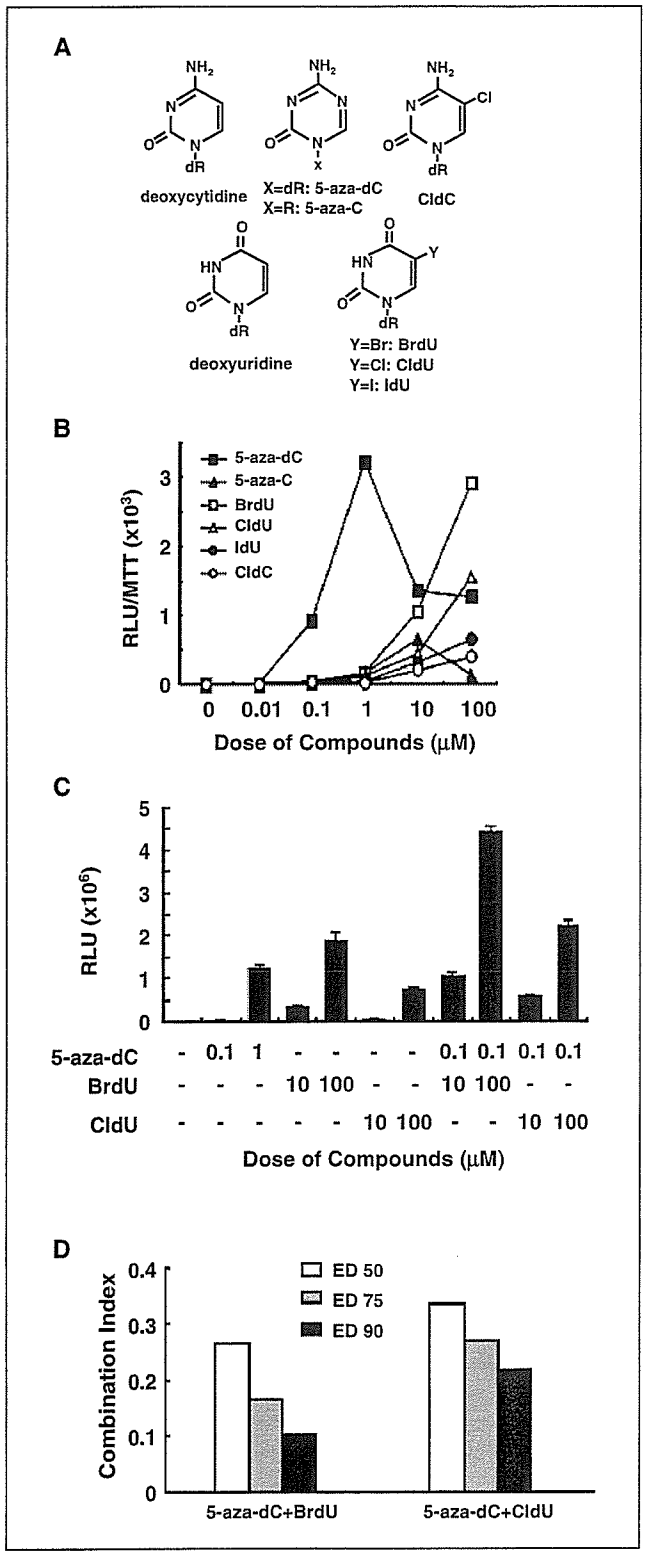

Figure 2. Identification of a group of thymidine analogues as silencing inhibitors. *A*, chemical structures of deoxycytidine, deoxyuridine, and their analogues. *dR*, deoxyribose. *B*, antisilencing activity of the identified compounds unraveled by the method described in Fig. 1*D*. *C*, combination effect of 5-aza-dC and halogenated deoxyuridines. K5 cells were cultured in the presence of a single dose or a combination of compounds for 3 days followed by single-tube luciferase assay. *Columns*, mean from triplicate wells; bars, SD. *D*, dose effect analysis. K5 cells were concomitantly exposed to 5-aza-dC and BrdUrd or CldU for 3 days. Luciferase activity was measured by 96-well plate luciferase assay. The CI was determined by the method based on the computer software Calcusyn. Data plotted are CI values at 50%, 75%, and 90% fractions of luciferase induction (ED). CI < 1, CI = 1, and CI > 1 indicate synergism, additive effect, and antagonism, respectively.

Antisilencing activity of halogenated thymidines is not associated with DNA demethylation. To clarify the mechanisms of antisilencing activities observed in halogenated thymidines, DNA methylation in the promoter region of reporter gene and *GSTP1* gene was examined by bisulfite genomic sequencing. The retroviral 5′-LTR promoter region in K5 cells cultured without G418 (K5/−) was hypermethylated (77%), whereas almost no methylation was detected in K5 cells cultured with G418 (K5/+; Fig. 4*A*). 5-Aza-dC significantly decreased the numbers of methyl-CpG to 34%, which was directly associated with the up-regulated luciferase activity. In contrast, BrdUrd and CldC did not demethylate hypermethylated retroviral promoter although they restored the silenced luciferase gene transcription (Fig. 4*A*). Similarly, BrdUrd did not influence the methylation status of the endogenous *GSTP1* promoter (Fig. 4*B*), whereas 5-aza-dC decreased DNA methylation. Our results showed that halogenated thymidines could activate a hypermethylated promoter by targeting processes other than DNA methylation.

Effect of halogenated thymidines on binding of methyl-CpG binding domain to methylated DNA. It is generally thought that promoter DNA methylation is translated to transcriptional silencing by a family of methyl-CpG binding domain proteins, which bind to methylated DNA through the evolutionarily conserved methyl-CpG binding domain (1). It is possible that incorporated halogenated thymidines disturb the binding of MBD to methyl-CpG sites, resulting in the antisilencing effect. The effect of halogenated thymidines on binding of MBD with methylated DNA was analyzed by gel shift assay using an artificially designed 20 bp double-stranded oligonucleotide probe containing two symmetrically methylated CpG sites with all thymidines replaced by BrdUrd (Fig. 5*A*). BrdUrd incorporation did not affect its binding to a recombinant MBD (Fig. 5*B*). Similar results were obtained when all thymidines were substituted with IdU in gel shift assay (data not shown). It is unlikely that BrdUrd disturbs MBD binding before incorporation into DNA because addition of the monophosphate or triphosphate form of BrdUrd into the protein-DNA binding reaction mixture did not influence the results in our gel shift experiment (data not shown). Taken together, BrdUrd did not disturb the binding of the methyl-CpG binding domain of MBD1 protein with methylated DNA *in vitro*.

Effect of 5-bromo-2′-deoxyuridine on histone modification. DNA methylation is usually associated with changes in the modifications of histone tails, which establish and maintain an inactive chromatin structure (27, 28). To clarify the antisilencing mechanism of BrdUrd, we did quantitative ChIP assay to detect changes in histone modification after BrdUrd treatment. Because acetylation of histone lysine tail is generally associated with

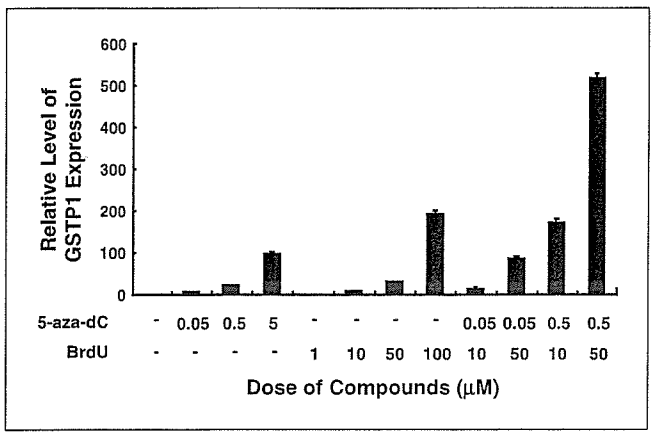

Figure 3. Reactivation of endogenous *GSTP1* gene transcription in MCF7 cells by BrdUrd. MCF7 cells were cultured in medium containing increasing amount of 5-aza-dC or BrdUrd or a combination of both drugs for 3 days. Expression of *GSTP1* gene was analyzed by quantitative real-time PCR assay.

transcriptional active chromatin (29), histone H3 acetylation of the retroviral promoter was studied. K5 cells maintained in G418 selection medium (K5/+) were used as a control, in which retroviral promoter sustained an active transcription state during long-term culture. As shown in Fig. 6*A*, K5/− cells exhibited decreased level of histone H3 acetylation in the retroviral promoter region compared with K5/+ cells, suggesting histone deacetylation in the proviral silencing. By exposing K5/− cells to BrdUrd for 3 days, histone H3 acetylation of the retroviral promoter recovered to a level comparative to that in K5/+ cells (Fig. 6*A*). On the other hand, the close linkage between methylation of histone H3 Lys[9] (H3K9) and transcriptional silencing has been reported (30, 31). In silenced K5/− cells, H3K9 in the retroviral promoter has been methylated (Fig. 6*B*). Treatment with 5-aza-dC or BrdUrd diminished this methylation. Thus, BrdUrd increased acetylation of histone H3 and decreased methylation of H3K9 along with intact DNA methylation.

Discussion

In this study, an MLV-based retroviral vector was used to establish a screening system for antisilencing compounds. This system successfully identified compounds with antisilencing activity. Although it has been reported that silenced retroviral vector becomes resistant to antisilencing agents during passage (32), the responsiveness of K5 cells to 5-aza-dC persisted for >6 months (data not shown). It is noteworthy that clones derived from MCF7 cells respond to TSA, but not to 5-aza-dC, which indicates that silencing of the retroviral promoter in these clones is not associated with DNA methylation, but is correlated with histone deacetylation. Indeed, the promoter region of the reporter gene in a MCF7 clone was not methylated at all (data not shown). This clone will be useful to screen compounds with antisilencing activity that is not associated with DNA methylation.

With this system, a group of halogenated thymidine analogues was identified as silencing inhibitors, which could activate the transcription of silenced genes without DNA demethylation. This is in agreement with the previous observation that BrdUrd-containing genome, even at very high substitution level, had no change in the content of 5-methylcytosine (33). In addition, BrdUrd has been shown to induce the expression from silenced endogenous

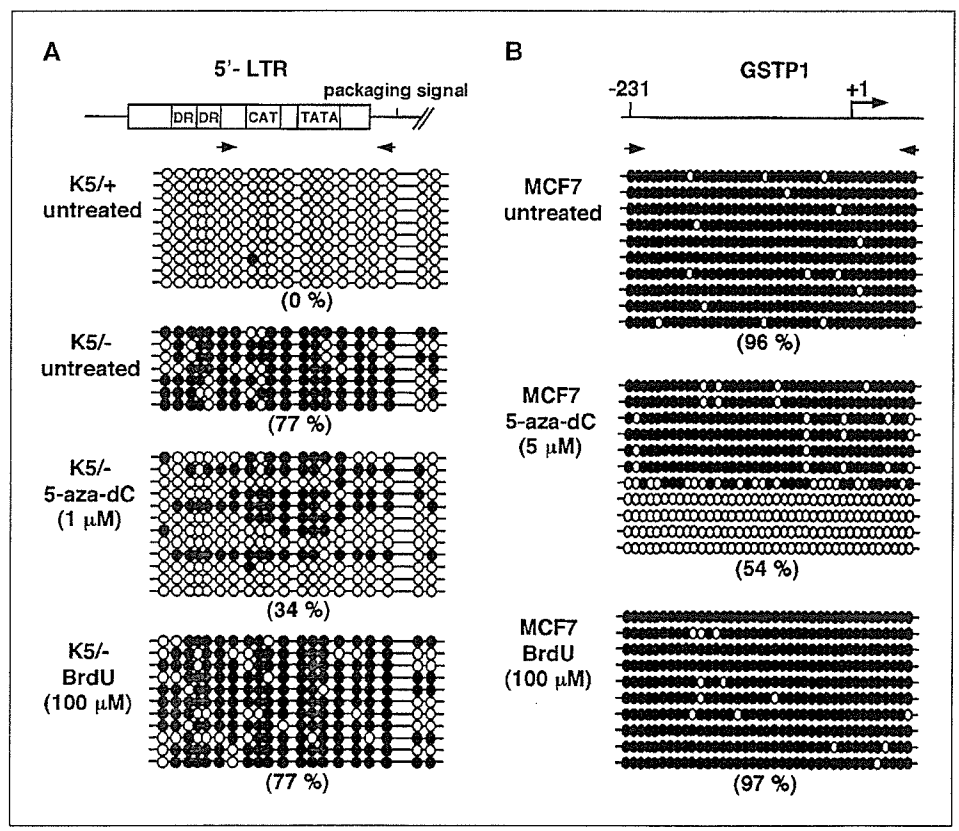

Figure 4. Bisulfite genomic sequencing for the effect of BrdUrd treatment on DNA methylation. *A*, CpG methylation of the retroviral promoter in K5 cells. *B*, methylation of the endogenous *GSTP1* promoter in MCF7 cells. K5 cells (*A*) or MCF7 cells (*B*) were treated with 5-aza-dC, BrdUrd, or CldU for 3 days. Genomic DNA was extracted and subjected to bisulfite genomic sequencing assay. *K5/+*, K5 cells maintained in G418 selection medium; *K5/−*, K5 cells cultured without G418. The analyzed region is shown at the top of each panel. *DR*, direct repeats of enhancer; *CAT*, CAT box; *TATA*, TATA box (39). *Arrows*, location of PCR primers. Open circles indicate unmethylated CpG whereas closed circles indicate methylated CpG. Percentages of methylated CpG sites among total CpG sites are shown in the parenthesis.

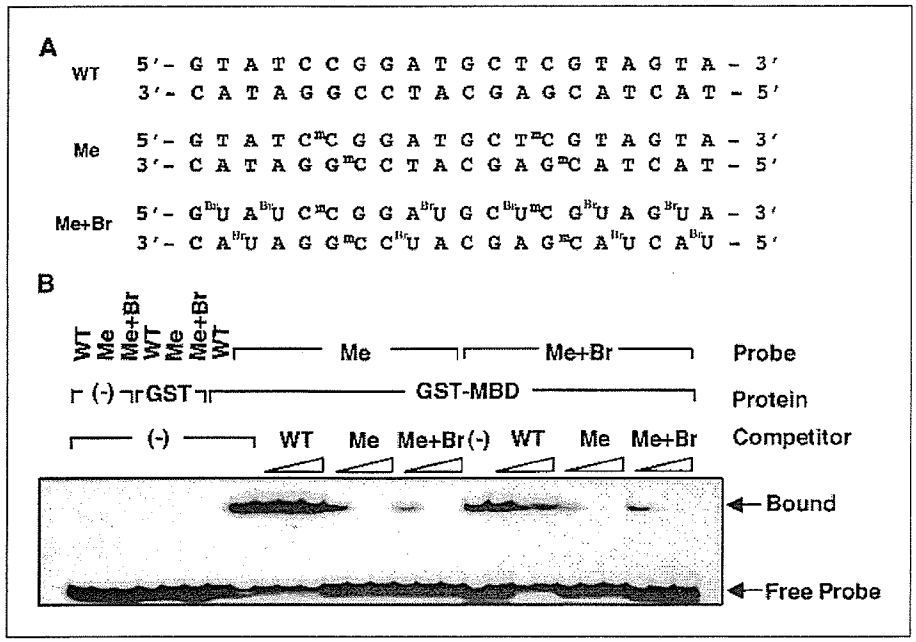

Figure 5. Binding of BrdUrd-incorporated DNA with methyl-CpG binding domain. *A*, oligonucleotides used in gel mobility shift assay. ^{m}C represents 5-methylcytosine. ^{Br}U represents bromouracil. *B*, gel mobility shift assay with GST-tagged recombinant MBD of MBD1 protein (GST-MBD). Triangles indicate an increasing amount of competitors (10-, 100-, and 1,000-fold relative to the probes).

retrovirus without effect on DNA methylation (34), which was also consistent with our findings. However, DNA methylation has not been studied regarding endogenous genes after treatment with BrdUrd. This study first showed that these halogenated thymidines reactivated the transcription of not only retrovirus, but also a heavily methylated endogenous gene. In addition, halogenated thymidines could not reactivate the transcription from the viral promoter in MCF7 clones (data not shown), which could respond to TSA but not to 5-aza-dC, suggesting that the antisilencing effects of halogenated thymidines are closely linked with DNA methylation. This finding coincides with the observation that BrdUrd could reactivate the transcription of endogenous *GSTP1* gene silenced by DNA hypermethylation in MCF7 cells, implicating that halogenated thymidines interfere with cellular protein(s) that function between methylated CpG and HDACs.

Several lines of evidence have indicated that DNA demethylation is not a prerequisite for the reactivation of heavily methylated loci. In helper T cells, GATA3 seems to activate interleukin-4 expression from a hypermethylated promoter by interfering with MBD2 binding to its target CpG sites without altering DNA methylation (35). Similarly, Lembo et al. (36) recently reported that MBDin, a regulatory factor of MBD2, reversed MBD2-mediated transcriptional repression from a methylated promoter by binding with the COOH-terminal region of MBD2. Another example of antisilencing without DNA demethylation has been shown in plants (37). *MOM* is an *Arabidopsis* gene that has been found to be important in maintaining gene silencing in a methylation-independent fashion. Suppression of its expression by siRNA reactivated the transcription of the genes, which existed in several densely methylated loci. It has been reported that BrdUrd-substituted DNA has changed its interaction with some chromatin and nonchromatin proteins (38), showing the possibility that incorporated halogenated thymidines activate transcription by interfering with the function of cellular proteins that are associated with DNA methylation–mediated gene silencing.

The synergistic effects of halogenated thymidines with 5-aza-dC also indicate that the mechanism of halogenated thymidines differs from that of 5-aza-dC. In spite of retained DNA methylation, the level of histone H3 acetylation was increased when treated by

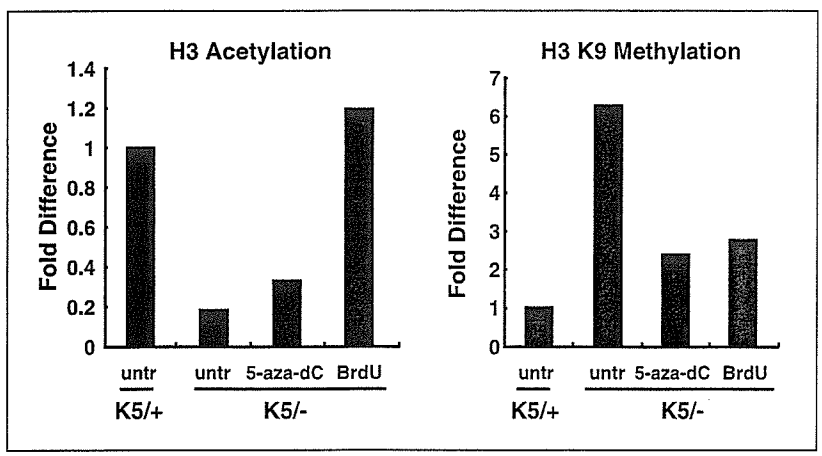

Figure 6. Quantitative ChIP assay for histone acetylation and methylation status of the retroviral promoter in K5 cells. K5 cells cultured in either G418 selection medium (K5/+) or nonselection medium (K5/−) were subjected to ChIP assay after exposure to 5-aza-dC or BrdUrd for 3 days using antiacetylated histone H3 antiserum (*A*) or antidimethyl histone H3 Lys^{9} (*B*). The presented diagram shows the fold difference of acetylated or methylated histone H3, where the data from K5/+ cells was arbitrarily set as 1.0. Three independent ChIP experiments have been done and a representative data is shown.

halogenated thymidines, indicating that these compounds impair the pathway by which DNA methylation is translated into histone deacetylation. Because *in vitro* experiments in this study showed that halogenated thymidines had no effect on the binding of the methyl-CpG binding domain with methylated DNA, they are considered to interfere with some steps downstream of MBDs. Further studies will be needed to clarify the antisilencing mechanism of these compounds.

The findings that halogenated thymidines have a different antisilencing mechanism from and show remarkable synergistic effects with 5-aza-dC raise possibilities that halogenated thymidines could become attractive lead compounds in treatments of cancers. Furthermore, this study implicates a new mechanism of halogenated thymidines that interfere with step(s) between DNA methylation and histone acetylation.

Acknowledgments

Received 9/30/2004; revised 4/8/2005; accepted 5/18/2005.

Grant support: Scientific Research from the Ministry of Education, Science, Sports and Culture of Japan.

The costs of publication of this article were defrayed in part by the payment of page charges. This article must therefore be hereby marked *advertisement* in accordance with 18 U.S.C. Section 1734 solely to indicate this fact.

We thank Shinjiro Hino for the valuable suggestions and discussions and Suzuko Osako for technical assistance.

References

1. Bird AP, Wolffe AP. Methylation-induced repression—belts, braces, and chromatin. Cell 1999;99:451–4.
2. Jones PA, Laird PW. Cancer epigenetics comes of age. Nat Genet 1999;21:163–7.
3. Baylin SB, Herman JG. DNA hypermethylation in tumorigenesis: epigenetics joins genetics. Trends Genet 2000;16:168–74.
4. Jones PA, Baylin SB. The fundamental role of epigenetic events in cancer. Nat Rev Genet 2002;3:415–28.
5. Egger G, Liang G, Aparicio A, Jones PA. Epigenetics in human disease and prospects for epigenetic therapy. Nature 2004;429:457–63.
6. Issa JP. Decitabine. Curr Opin Oncol 2003;15:446–51.
7. Ballestar E, Wolffe AP. Methyl-CpG-binding proteins. Targeting specific gene repression. Eur J Biochem 2001;268:1–6.
8. Slack A, Bovenzi V, Bigey P, et al. Antisense *MBD2* gene therapy inhibits tumorigenesis. J Gene Med 2002;4:381–9.
9. Sansom OJ, Berger J, Bishop SM, Hendrich B, Bird A, Clarke AR. Deficiency of MBD2 suppresses intestinal tumorigenesis. Nat Genet 2003;34:145–7.
10. Christman JK. 5-Azacytidine and 5-aza-2′-deoxycytidine as inhibitors of DNA methylation: mechanistic studies and their implications for cancer therapy. Oncogene 2002;21:5483–95.
11. Kantarjian HM, O'Brien S, Cortes J, et al. Results of decitabine (5-aza-2′deoxycytidine) therapy in 130 patients with chronic myelogenous leukemia. Cancer 2003;98:522–8.
12. Goffin J, Eisenhauer E. DNA methyltransferase inhibitors—state of the art. Ann Oncol 2002;13:1699–716.
13. Hurd PJ, Whitmarsh AJ, Baldwin GS, et al. Mechanism-based inhibition of C5-cytosine DNA methyltransferases by 2-*H* pyrimidinone. J Mol Biol 1999;286:389–401.
14. Cheng JC, Matsen CB, Gonzales FA, et al. Inhibition of DNA methylation and reactivation of silenced genes by zebularine. J Natl Cancer Inst 2003;95:399–409.
15. Cheng JC, Weisenberger DJ, Gonzales FA, et al. Continuous zebularine treatment effectively sustains demethylation in human bladder cancer cells. Mol Cell Biol 2004;24:1270–8.
16. Satou Y, Nosaka K, Koya Y, Yasunaga JI, Toyokuni S, Matsuoka M. Proteasome inhibitor, bortezomib, potently inhibits the growth of adult T-cell leukemia cells both *in vivo* and *in vitro*. Leukemia 2004;18:1357–63.
17. Chou TC, Talalay P. Analysis of combined drug effects: a new look at a very old problem. Trends Pharmacol Sci 1983;4:450–4.
18. Chou J. Quantitation of synergism and antagonism of two or more drugs by computerized analysis. In: Chou TC, Rideout DC, editors. Synergism and antagonism in chemotherapy. San Diego (CA): Academic Press; 1991. p. 223–44.
19. Nosaka K, Maeda M, Tamiya S, Sakai T, Mitsuya H, Matsuoka M. Increasing methylation of the *CDKN2A* gene is associated with the progression of adult T-cell leukemia. Cancer Res 2000;60:1043–8.
20. Wang L, Groves MJ, Hepburn MD, Bowen DT. Glutathione *S*-transferase enzyme expression in hematopoietic cell lines implies a differential protective role for T1 and A1 isoenzymes in erythroid and for M1 in lymphoid lineages. Haematologica 2000;85:573–9.
21. Mutskov V, Felsenfeld G. Silencing of transgene transcription precedes methylation of promoter DNA and histone H3 lysine 9. EMBO J 2004;23:138–49.
22. Ohki I, Shimotake N, Fujita N, et al. Solution structure of the methyl-CpG binding domain of human MBD1 in complex with methylated DNA. Cell 2001;105:487–97.
23. Fraga MF, Ballestar E, Montoya G, Taysavang P, Wade PA, Esteller M. The affinity of different MBD proteins for a specific methylated locus depends on their intrinsic binding properties. Nucleic Acids Res 2003;31:1765–74.
24. Hino S, Fan J, Taguwa S, Akasaka K, Matsuoka M. Sea urchin insulator protects lentiviral vector from silencing by maintaining active chromatin structure. Gene Ther 2004;11:819–28.
25. Yoshida M, Kijima M, Akita M, Beppu T. Potent and specific inhibition of mammalian histone deacetylase both *in vivo* and *in vitro* by trichostatin A. J Biol Chem 1990;265:17174–9.
26. Lin X, Nelson WG. Methyl-CpG-binding domain protein-2 mediates transcriptional repression associated with hypermethylated GSTP1 CpG islands in MCF-7 breast cancer cells. Cancer Res 2003;63:498–504.
27. Richards EJ, Elgin SC. Epigenetic codes for heterochromatin formation and silencing: rounding up the usual suspects. Cell 2002;108:489–500.
28. Nan X, Ng HH, Johnson CA, et al. Transcriptional repression by the methyl-CpG-binding protein MeCP2 involves a histone deacetylase complex. Nature 1998;393:386–9.
29. Dillon N, Festenstein R. Unravelling heterochromatin: competition between positive and negative factors regulates accessibility. Trends Genet 2002;18:252–8.
30. Zhang Y, Reinberg D. Transcription regulation by histone methylation: interplay between different covalent modifications of the core histone tails. Genes Dev 2001;15:2343–60.
31. Nguyen CT, Weisenberger DJ, Velicescu M, et al. Histone H3-lysine 9 methylation is associated with aberrant gene silencing in cancer cells and is rapidly reversed by 5-aza-2′-deoxycytidine. Cancer Res 2002;62:6456–61.
32. McInerney JM, Nawrocki JR, Lowrey CH. Long-term silencing of retroviral vectors is resistant to reversal by trichostatin A and 5-azacytidine. Gene Ther 2000;7:653–63.
33. Singer J, Stellwagen RH, Roberts-Ems J, Riggs AD. 5-Methylcytosine content of rat hepatoma DNA substituted with bromodeoxyuridine. J Biol Chem 1977;252:5509–13.
34. Schwartz SA. Transcriptional activation of endogenous rat retrovirus with and without hypomethylation of proviral DNA. Biochem Biophys Res Commun 1983;112:571–7.
35. Hutchins AS, Mullen AC, Lee HW, et al. Gene silencing quantitatively controls the function of a developmental *trans*-activator. Mol Cell 2002;10:81–91.
36. Lembo F, Pero R, Angrisano T, et al. MBDin, a novel MBD2-interacting protein, relieves MBD2 repression potential and reactivates transcription from methylated promoters. Mol Cell Biol 2003;23:1656–65.
37. Amedeo P, Habu Y, Afsar K, Scheid OM, Paszkowski J. Disruption of the plant gene MOM releases transcriptional silencing of methylated genes. Nature 2000;405:203–6.
38. Fasy TM, Cullen BR, Luk D, Bick MD. Studies on the enhanced interaction of halodeoxyuridine-substituted DNAs with H1 histones and other polypeptides. J Biol Chem 1980;255:1380–7.
39. Graves BJ, Eisenman RN, McKnight SL. Delineation of transcriptional control signals within the Moloney murine sarcoma virus long terminal repeat. Mol Cell Biol 1985;5:1948–58.